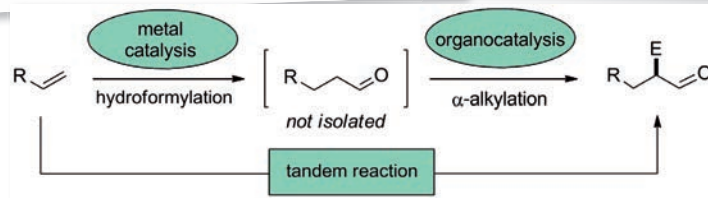
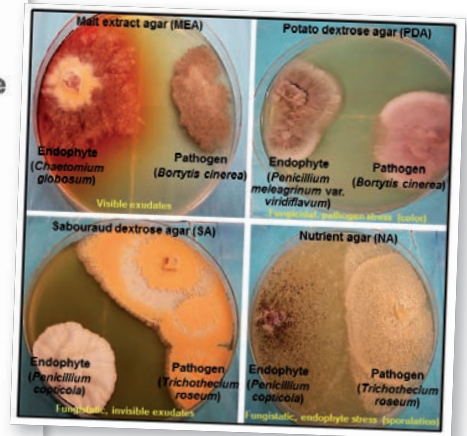
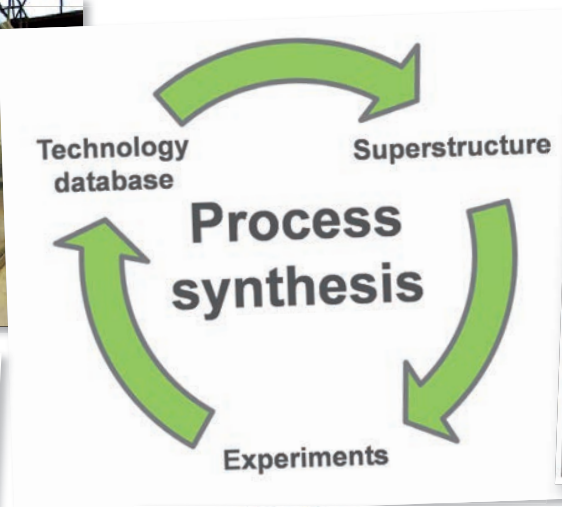
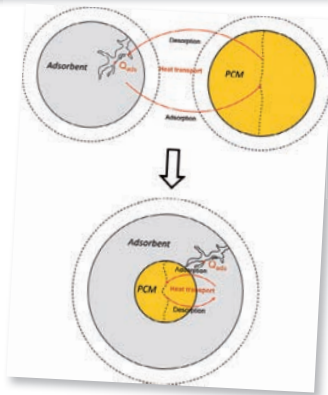


SCIENTIFIC HIGHLIGHTS

Annual Report



2012

Content

Department of BCI	4
Preface	5
Equipment Design (AD)	6
Mixing enhancement and continuous dispersion	7
Future production concepts in chemical industry	8
Improved Safety in Chemical Processes	9
Plant and Process Design (APT)	10
Chromatographic purification of natural products	11
Investigation of protein adsorption at the gas-liquid interface	12
Biomaterials and Polymer Science (BMP)	14
Nanocontainers based on hyperbranched Polylysine	15
Biocatalyzed reactions in APCN particles in organic solvents	16
Poly(2-oxazoline) based amphiphilic polymer conetworks	17
New Materials for Energy Storage	18
Extending the Limits of Shape Memory Polymers	19
Chemical Biotechnology (BT)	20
Biocatalytic gram-scale production of (S)-limonene	21
Characterization of a proline-hydroxylating whole-cell biocatalyst	22
A new chassis for industrial biotechnology: <i>Pseudomonas taiwanensis</i> VLB120	23
Biochemical Engineering (BVT)	24
Immobilization of tyrosinase in alginate matrix capsules	25
Scale-Up of the production of Biosurfactants	26
Chemical Reaction Engineering (CVT)	28
Energy-efficient adsorptive CO ₂ -capture from cement flue gas	29
Capillary microreaction engineering	30
Process Dynamics and Operations (DYN)	32
Monitoring emulsion polymerisations by ultra-sound velocity	33

Content

Fluid Separations (FVT)	34
Process intensification for CO ₂ capture processes	35
Reactive Extraction	36
Mechanical Process Engineering (MV)	38
Auto-conveying probing-apparatus for extraction of particle free samples from process gasses	39
Transportation of thin fluid films by pulsation	40
Fluid Mechanics (SM)	42
Microfluidics	43
Two-phase micro-reactors	44
Liquid-particle micro-flow	45
Technical Biochemistry (TB)	46
Localisation and detection of cannabinoids in isolated <i>C. sativa</i> L. trichomes	47
Endophytes – the plant-associated microbial treasure troves	48
Technical Chemistry - Chemical Process Development (TC)	50
Oxygen depolarized cathodes with electrodeposited catalyst	51
Generating primary amines in an aqueous biphasic medium	52
Ethenolysis of castor oil derivatives	53
Linear oligomerization of 1-butene with a homogeneous catalyst system based on allylic nickel complexes	54
Enantioselective Tandem Reactions at Elevated Temperatures	55
Thermodynamics (TH)	56
Modelling of hydrogel networks	57
Thermodynamics of biological reactions	58
Thermodynamic Characterization of Ionic Liquid Solutions	59
Integrated Chemical Processes in Liquid Multiphase Systems (InPROMPT)	60
APT/DYN: A framework for the modeling and stochastic optimization of process superstructures under uncertainty	61
FVT: Graphical design tools for Organic Solvent Nanofiltration	62
TC: Rhodium Catalyzed Hydroformylation of 1-Dodecene	63
TH: Melt crystallization of isomeric long-chain aldehydes	64



Department of BCI

Preface

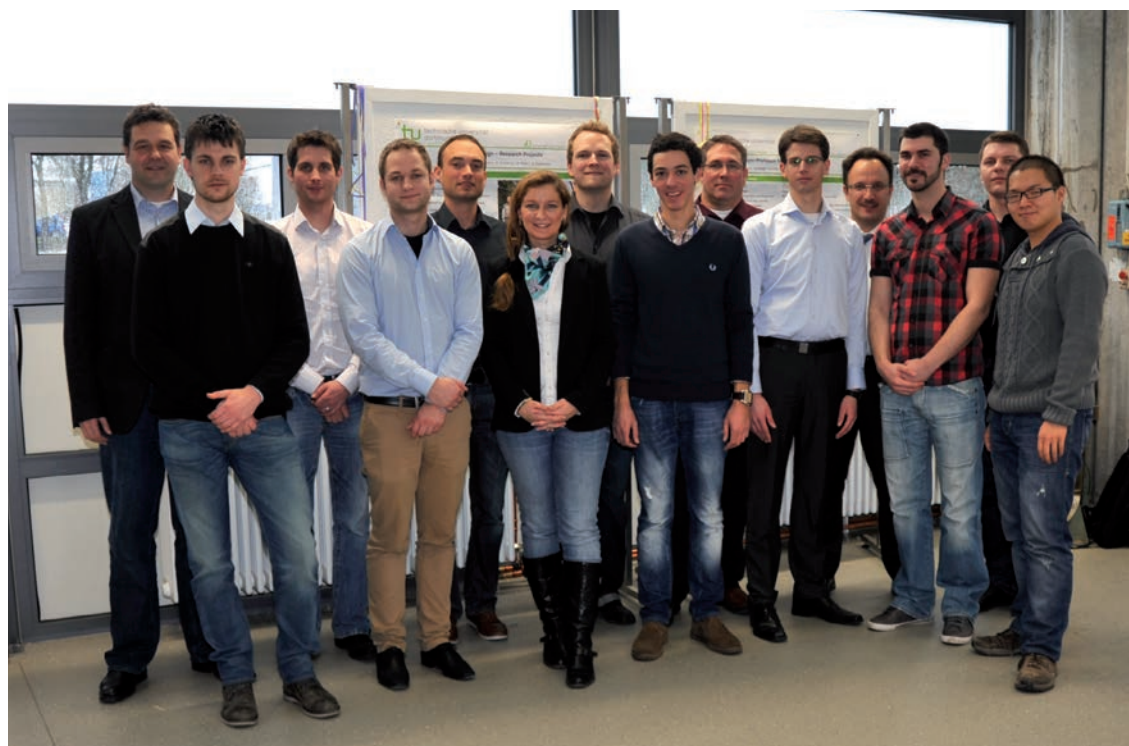
Dear Readers,

the year 2012 has been very successful for the department of bio- and chemical engineering. Again, the great diversity of the faculty has brought numerous scientific insights into technical and natural processes and materials, advanced separation and production techniques in chemical and biochemical engineering, and ways to describe and control those most complex processes. Particularly, the possibility of collaborating between the various disciplines of the half natural science and half engineering science chairs has enabled this success.

The here presented Scientific Highlights are not only examples for the successful work, but should also serve the purpose of further strengthening these collaborations between the groups and also with scientist from other departments of the TU Dortmund and with scientist from other universities and industry.

Further, we hope that reading the highlights might encourage students from everywhere to join the research at BCI as Ph.D. students or Postdocs. Particularly, the existing graduate schools are always looking for motivated candidates.

Enjoy the reading.



Equipment Design (AD)

Mixing enhancement and continuous dispersion

Intensified processes in complex microchannels

Alexander Holbach, Norbert Kockmann

Homogeneous mixing of liquids in microchannels is well known and characterized for simple channel geometries. Also meandering mixing channels, in which Dean vortices are generated, are often employed to achieve rapid mixing of liquids. Our studies aim to increase the mixing performance in the contacting and first mixing elements. Dean vortices in the inlet channels improve the mixing quality for Reynolds numbers in the range from $Re = 20$ to 200 together with S-shaped mixing elements. This enhancement was also found in two-phase flow.

Starting from a T-mixer and a Tangential mixer, the contact element was varied from Twisted-Y mixer to 60° Y mixer. The mixing quality was increased during the optimization study and was very high for the 60° Y-mixer after one single SZ mixing channel element for Re numbers larger than 200 . Curved inlet channels do not significantly enhance the mixing performance.

The residence time distribution is an important parameter for chemical reactors and was simulated for the improved mixing structures. It shows a characteristic between the two models of pure convection and dispersion in the Tangential and 60° Y mixer. Due to the increasing strength of secondary flow structures, the residence time distribution approaches the prediction of the axial dispersion model with increasing Re number. For the range of $100 < Re < 500$, the residence time characteristic cannot be predicted with sufficient accuracy by one of the models. The tolerable degree of backmixing in the mixing channel depends on the chemical reaction to be performed in the micromixer.

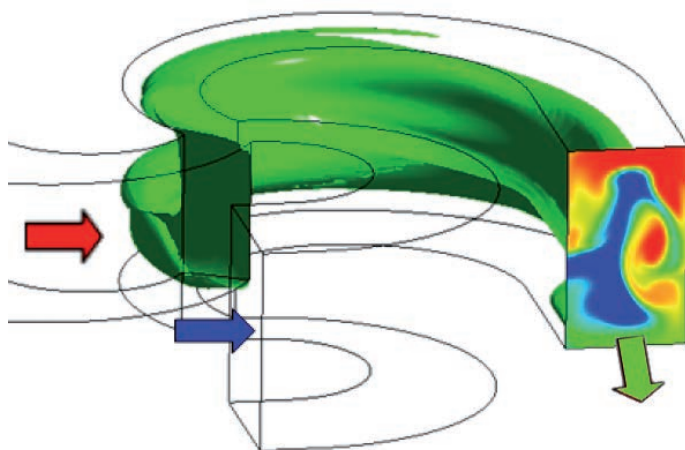


Figure 1: Concentration profiles in contactor and after first bend in the Twisted-Y mixer with equal inlet heights at $Re = 250$.

Contact:
alexander.holbach@bci-tu-dortmund.de
kockmann@bci-tu-dortmund.de

On the base of the convective flow studies in microchannels two-phase liquid flow was also investigated. The entire device consists of a droplet generator, a channel to enable an intensified mass transfer between the two fluids and a liquid-liquid separation device. Experiments were carried out with deionized water as continuous phase and various organic solvents as dispersed phase. The organic droplets are generated by direct co-flowing injection through a needle located in the center of the microchannel. Droplet generation and flow patterns were optically investigated in straight channels. The mass transport was studied by a fast acid-base neutralization reaction in straight and winding channels. Channel curvature increases dramatically the mass transfer in the continuous phase, see Fig. 2 c).

The adjacent separation unit continuously splits the organic, disperse phase. Combined effects of gravity, wetting characteristics of the wall material, and capillary forces nearly completely separate the two fluids over a wide range of flow rates. Based on the mixer-settler system, a microfluidic extraction unit is proposed, which enables a multistage counter-current arrangement.

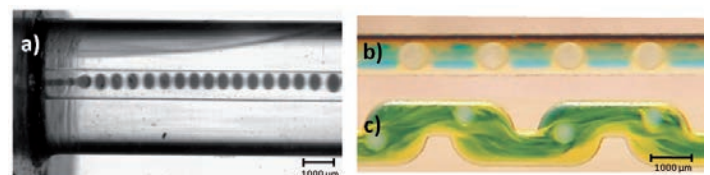


Figure 2: Concentration profiles in contactor and after first bend in the Twisted-Y mixer with equal inlet heights at $Re = 250$.

Publications:
Holbach, N. Kockmann, Kontinuierliches Mixer-Settler-Konzept für die Tropfenströmung in mikrostrukturierten Kanälen, Chemie-Ingenieur-Technik, 84, 1398, 2012.
M. Fischer, N. Kockmann, Enhanced convective mixing and residence time distribution in advanced micro-mixers, ASME-ICNMM2012-73275, Puerto Rico, July 8, 2012.
P. Plouffe, R. Anthony, A. Donaldson, D.M. Roberge, A. Macchi, N. Kockmann, Transport phenomena in two-phase liquid-liquid microreactors, ASME-ICNMM2012-73040, Puerto Rico, July 8, 2012.

Improved Safety in Chemical Processes

Process development of exothermic reactions

Norbert Kockmann

Closed handling, enhanced heat transfer, and the small internal volume of microreactors allow for safe processing of challenging and hazardous reactions. Besides a robust and scalable reactor, pumps, vessels, and separation units have to be considered in the safety concept. Typical chemical reactions embrace organometallic reactions and nitration. With check lists the systematic approach is assisted in the risk assessment on the basis of the HAZOP method.

Safe processing of hazardous, rapid, and strongly exothermic chemical reactions in microchannels is often the main motivation to apply microreactors. High rates in mixing, mass and heat transfer as well as the small internal volume allow novel process windows with often harsh reaction conditions of high temperature or concentrations. However, good results from laboratory studies must be brought to pilot and production scale for economical success of a product and its related process. One key factor of the reactor scale-up is the specific channel design for fast mixing and additionally sufficient volume for residence time under controlled temperature conditions. The design must also provide sufficient geometric similarity over the entire scale the process is developed and operated.

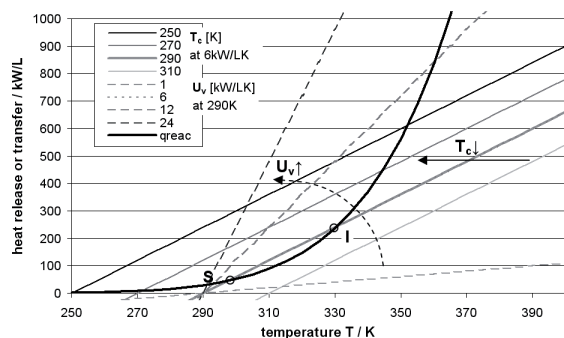


Figure 1: Semenov curve for exothermic reactions with generated and dissipated heat.

Furthermore for strong exothermic reactions, the parametric sensitivity and reactor stability is a crucial issue, which is determined by reaction kinetics and thermodynamics and the heat transfer capacity of the reactor. The generated heat from the chemical reaction must be dissipated to the cooling media, see Fig. 1. Beside the improved heat transfer in microchannels, splitting up

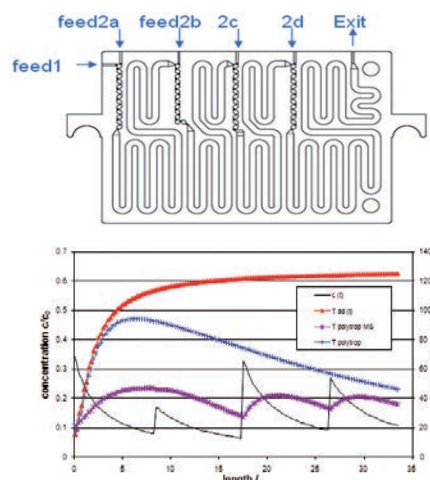


Figure 2: Principle of the multiinjection plate (Lonza Flowplate™) with four inlets and mixing zones (top) and lower temperature profile compared to single mixing element (bottom).

the reagents leads also to a lower temperature profile and safe reaction conditions, see Fig. 2.

After successful laboratory campaign and in preparation of the scale-up, the following procedure is recommended to determine process conditions and reactor setup for higher throughput and production rates.

- determine flow rate, pressure drop, and related Re number in the mixing and residence channel for the reactor set up in the lab,
- check heat transfer and reaction kinetics to determine,
- calculate the limiting flow rate for laminar flow and determine diameters for turbulent regime,
- with extrapolating the hydraulic diameter to the higher flow rate, the reactor size can be determined,
- check, whether mixing or heat transfer is the limiting process.

Residence time of the fluids in the reactor should always be in the same order of magnitude to guarantee complete conversion.

The above mentioned criteria give a first estimation and should be enlarged to embrace the complexity of a real chemical system. The references give more details on the scale-up process and related design considerations.

Publications:

N. Kockmann, Sicherheitsaspekte bei der Prozessentwicklung und Kleinmengenproduktion mit Mikroreaktoren, Chemie-Ingenieur-Technik, 84, 715-726, 2012.
N. Kockmann, Safe reaction conditions and their scale-up in microstructured reactors, IMRET12, Lyon, February 20-22, 2012.

Contact:

kockmann@bci.tu-dortmund.de

Future production concepts in chemical industry

Thomas Bieringer, Norbert Kockmann

Microstructured reactors have found their role in laboratories for analytical and chemical synthesis purposes. To bring the lab results into production, the process has to be scaled up for higher throughput. A modular setup of the process steps such as heat exchange, mixing, or sufficient residence time under controlled process conditions is very helpful during scale up and for rapid process development. The platform concept of devices with similar flow rates and process conditions gives a robust framework for consistent scale up.

A key concept of process intensification is to treat molecules in an optimal way during the entire process. To achieve this ambitious goal, unit operations can be replaced by unit functions and functional modules to find a basic route of a chemical process. It is widely accepted that microreactors play an integral part of process intensification. Physical and chemical parameters can be determined in small devices with low consumption of precious materials from fine chemistry and pharmaceutical development. Typical characteristics of these continuous-flow devices and processes are short mixing time, excellent heat transfer and controlled residence time with small internal hold-up.

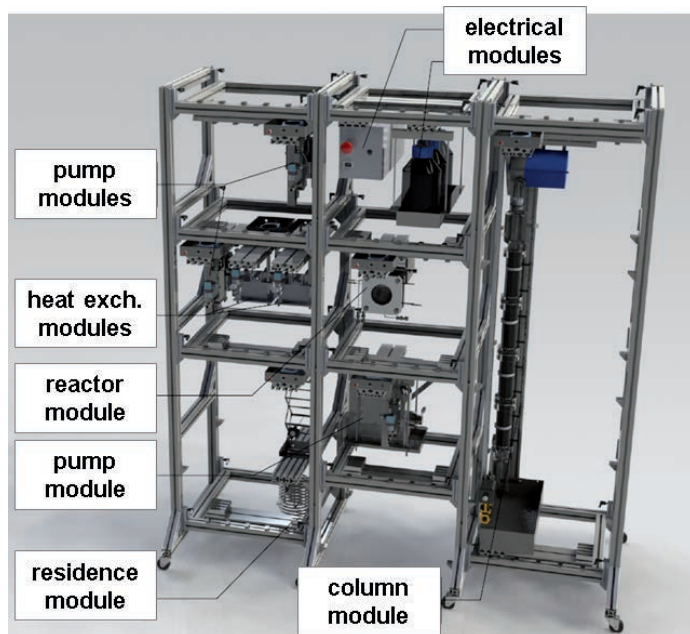


Figure 1: Modular setup of lab equipment for a chemical reaction with adjacent extraction step.

To bring the lab results into production, we have developed a modular reactor and continuous-flow plant setup, see Fig. 1. Different unit functions can be realized in a flexible plant configuration for various process conditions. The modular equipment setup is assisted by an integrated platform concept for consistent scale-up and early small scale production campaigns, see Fig. 2.

Contact:
kockmann@bci.tu-dortmund.de

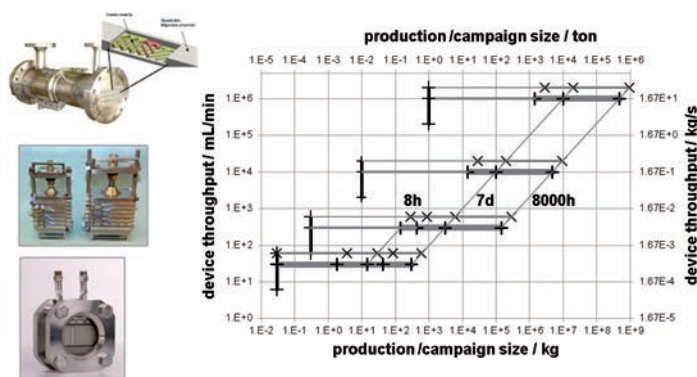


Figure 2: Platform concept and scale-up of tubular reactors with examples of Lonza FlowPlate™ reactor and Ehrfeld BTS GmbH Miprowa devices. The process time is the dominant factor for high production rates.

The modular setup of process equipment already in the laboratory enables the investigation of chemical processes and unit steps for intensified and consistent process development. The modules are often related to existing equipment and allow for a versatile plant configuration. The scale-up of the lab results follow the platform concept with different levels of volumetric flow rate (module size, see Fig. 2), temperature, pressure, and chemical resistivity. The same modules have similar characteristics on different platform levels and minimize the risk of process scale-up to production. The goal of this concept is the extensive process development and already detail engineering in the lab phase of process design. This enables a rapid market supply of small and medium amount of chemical products. The collaboration of TU Dortmund, BCI with Bayer Technology Services BTS in the research platform INVITE GmbH enables the development and practical testing of modular equipment.

Publications:

- N. Kockmann, Modular microstructured reactors with integrated platform concept, *Procedia Engineering*, CHISA 2012
- N. Kockmann, T. Bieringer, Forschungsplattform INVITE – Beschleunigte Prozessentwicklung vom Labor in die Produktion, *Chemie-Ingenieur-Technik*, 84, 1227-1228, 2012.
- N. Kockmann, J. Kussi, G. Schembecker, Die 50%-Idee: vom Produkt zur Produktionsanlage in der halben Zeit, *Chemie-Ingenieur-Technik*, 84, 563, 2012.
- N. Kockmann, Scale-up-fähiges Equipment für die Prozessentwicklung, *Chemie-Ingenieur-Technik*, 84, 646-659, 2012.



Plant and Process Design (APT)

Chromatographic purification of natural products

New process design for purification of rebaudioside A from *Stevia rebaudiana* Bertoni leaves

Dominik Bergs, Juliane Merz, Axel Delp, Matthias Jöhnck, Georg Martin, Gerhard Schembecker

A chromatographic process idea for preparative purification of rebaudioside A from aqueous extracts of Stevia rebaudiana Bertoni leaves is developed. The process can handle high concentrated aqueous extracts, needs less equipment and has a lower solvent consumption compared to the state-of-the-art purification process of rebaudioside A.

In recent years, sweet diterpene glycosides of the shrub *Stevia rebaudiana* Bertoni have gained importance in food, cosmetic and pharmaceutical industries. Steviol glycosides are non-caloric sweeteners of up to 300 times the sweetness of sucrose, which makes them an attractive sugar substitute for food industry. There are over 30 steviol glycosides identified, whereas rebaudioside A has the greatest sensorial taste and is therefore the molecule of interest.

The state-of-the-art method for the purification of rebaudioside A from leaves of *Stevia rebaudiana* Bertoni involves a cascade of different unit operations and is shown in figure 1. Several filtration steps, a precipitation of undesired components, decolouration, anion and cation exchange, and finally a multi-stage crystallization process is necessary to get a final purity of 95 %. More than four solvent changes, some drying and resolving steps and the use of chelators are necessary for this process.

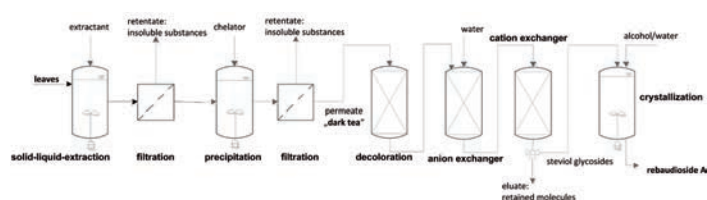


Figure 1: State-of-the-art process^[1] for separation of rebaudioside A from the leaves of *Stevia rebaudiana* Bertoni^[1]U. Kienle, J. Verbr. Lebensm. 5(2) 2010

The chromatographic process developed in this study is supposed to simplify the purification of rebaudioside A. The new process can handle highly concentrated aqueous extracts, requires less equipment, less solvent changes, needs no additives and can reach the required purity without any multi-stage unit operation.

The extraction of *Stevia rebaudiana* leaves is performed with water as extractant. After solid liquid separation, the crude extract is purified.

The new process consists of a cascade of three preparative chromatographic columns (cf. figure 2). The first column (P91 development product, Merck Millipore) separates steviol glycosides from the plant matrix using water as eluent in reversed phase mode. Thus, there is no solvent change necessary between aqueous extraction and the first chromatographic step. The fraction of steviol glycosides is then concentrated on a second column (Pharmprep® P100 RP-18e, Merck Millipore) which works as a capture column with a more non-polar adsorbent. Additionally, the capture

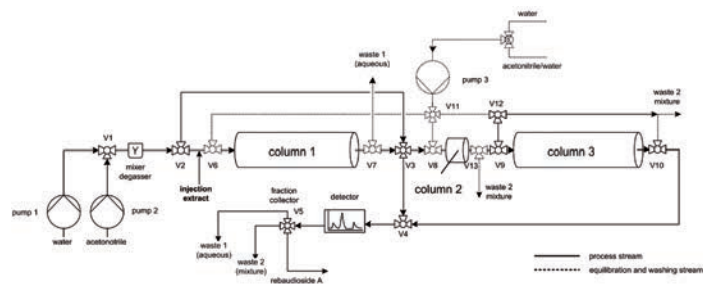


Figure 2: New process design for preparative separation of rebaudioside A from *Stevia rebaudiana* Bertoni leaves

step is used as a peak shaping and concentration step. The last column (LiChroprep NH₂, Merck Millipore) separates rebaudioside A from steviol glycoside under normal phase conditions using a mixture of acetonitrile and water as eluent. The new chromatographic process design increases the yield from 77 % to 97.5 % ± 1.5 %. With a purity of 96.8 % ± 1.4 % the process fulfills the legal requirements for the purity of rebaudioside A.

Contact:

Dominik.Bergs@bci.tu-dortmund.de

Juliane.Merz@bci.tu-dortmund.de

Gerhard.Schembecker@bci.tu-dortmund.de

Publications:

D. Bergs, J. Merz, A. Delp, M. Joehnck, G. Martin, G. Schembecker, Preparative purification of rebaudioside A from aqueous extracts using chromatography: a process idea, *Journal of Consumer Protection and Food Safety*, 7(4), 2012, p.295-303.
D. Bergs, J. Merz, A. Delp, M. Joehnck, G. Martin, G. Schembecker, Preparative separation of rebaudioside A from stevia leaves using inverted chromatographic process design - An overview, In: Geuns, Jan M.C. (Ed.), *Stevia: 6 months beyond authorisation*. Euprint, Heverlee, (2012) p.105-112, ISBN: 978-90-742-53208.
D. Bergs, B. Burghoff, A. Delp, M. Joehnck, G. Martin, G. Schembecker, Fast and isocratic HPLC-method for steviol glycosides analysis from *Stevia rebaudiana* leaves, *Journal of Consumer Protection and Food Safety*, 7(2), 2012, p.147-154.

Investigation of protein adsorption at the gas-liquid interface

Ivana Barackov, Juliane Merz, Gerhard Schembecker

Almost all proteins have an amphiphilic nature, which means that they can spontaneously adsorb at a gas-liquid interface. This property is used and applied in foam fractionation process for concentration or separation of proteins from protein-rich solutions. Protein adsorption to the interface can include orientation changes or even unfolding of the protein. To investigate the occurring structural and conformational changes at the gas-liquid interface a combination of different spectroscopic techniques was used.

Foam fractionation is a gentle, inexpensive and selective method for effective separation of surface active compounds, like proteins, from diluted solutions. For better elucidation of foam fractionation it is important to understand the behavior of proteins at the gas-liquid interface on molecular level. Therefore, a combination of different spectroscopic techniques was applied to characterize the protein behavior at the interface.

Different proteins like BSA, lysozyme, and β -casein were foamed in batch-mode. To detect irreversible structural changes after foam fractionation circular dichroism (CD) spectroscopy was performed. The initial feed solution and foamate (collapsed foam) were measured.

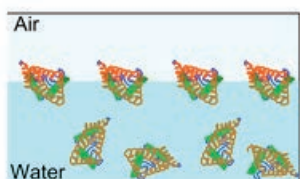


Figure 1: Schematic representation of likely arrangement of protein at the gas-liquid interface.

To obtain detailed molecular information of protein structure during adsorption infrared reflection adsorption spectroscopy (IRRAS) was used. This technique gives detailed molecular information about proteins at the gas-liquid interface and describes in situ changes of their secondary structure. Additionally, the surface pressure as a function of time was measured.

CD spectra showed no structural changes of foamed proteins after the foam fractionation. This means that all structural changes occurring during foam fractionation were reversible for the investigated proteins. According to the IRRAS spectra, however, it could be shown that flexible proteins, like β -casein and BSA, adsorb to the interface without significant change of structure. For less flexible and less hydrophobic proteins like lysozyme, the changes in the secondary structure during adsorption were significant.

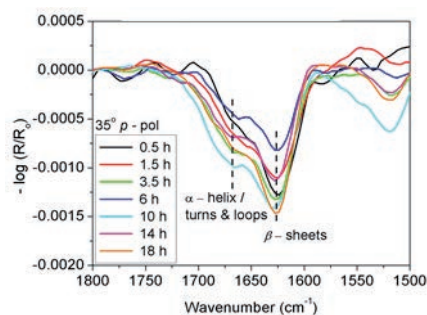


Figure 2: IRRAS spectra of lysozyme unfolding during adsorption to the gas-liquid interface.

Thus, flexible proteins possess the ability to adapt themselves to the interface by orientation only, without changing their structure. Less flexible or rigid proteins tend to partially unfold themselves reversible under certain conditions.

Publications:

Article:

I. Barackov, A. Mause, S. Kapoor, R. Winter, G. Schembecker, B. Burghoff. Investigation of structural changes of β -casein and lysozyme at the gas-liquid interface during foam fractionation, *Journal of Biotechnology*, 2012, vol. 161 (2), p. 138-146.

Oral presentation:

I. Barackov, S. Kapoor, R. Winter, G. Schembecker. Investigation of protein adsorption during foam fractionation by infrared reflection adsorption spectroscopy, *ProcessNet-Jahrestagung*, Karlsruhe (2012).

Contact:

ivana.barackov@bci.tu-dortmund.de
juliane.merz@bci.tu-dortmund.de
gerhard.schembecker@bci.tu-dortmund.de



Biomaterials and Polymer Science (BMP)

Nanocontainers based on hyperbranched Polylysine

Metal nanoparticle composites and non-toxic antimicrobial coatings with controlled release

Matthias Thiel, Chau Hon Ho, Jörg C. Tiller

Branched amphiphilic polymeric systems with core-shell architecture can be used as versatile nanocontainers and templates with great potential in application fields ranging from medicine to organic coatings. In order to explore an alternative to the already widely used and established synthetic macromolecules, we synthesized new polymers based on highly branched and hyperbranched polylysine (HPL). The PL was prepared with classical heating and microwave assisted.

A hyperbranched polylysine (DB = ca. 53%, $M_n = 10700$ g/mol and $M_w = 20500$ g/mol) was synthesized via thermal polycondensation under optimized conditions using lysine hydrochloride and sodium hydroxide as starting materials. This hydrophilic and biocompatible polyamine was hydrophobized via polymeranalog reactions using a mixture of stearyl/palmitoyl chloride (FA) and glycidyl hexadecyl ether (GHE), respectively.

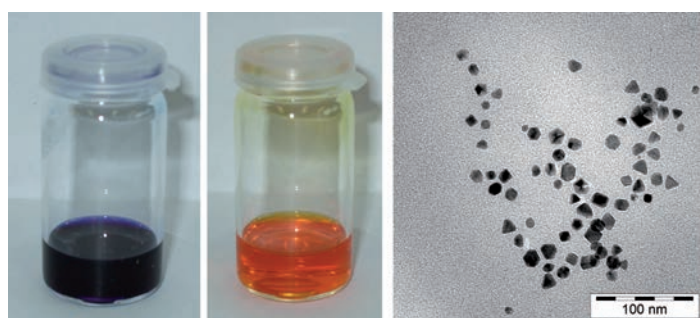


Figure 1: Photographs of solutions of organo-insoluble dyes in chloroform with hydrophobic HPL-nanocontainer and TEM image of Pd-nanocrystals formed within the nanocontainers.

The synthesized HPL derivatives GHE90-HPL and FS80-HPL are soluble in organic media, such as toluene and chloroform. Polymer solutions of GHE90-HPL in toluene allowed the solubilization of metal compounds (AgNO_3 , HAuCl_4 and Li_2PdCl_4) and supported the formation of metal nanoparticles (Ag, Au, Pd) when adding reducing agents such as L-ascorbic acid and $\text{Li}[\text{HBEt}_3]$. In case of the palladium reduction with L-ascorbic acid Pd nanocrystals were formed (Figure 1).

The hydrophobically-modified hyperbranched polylysine core-shell nanocontainer with silver nanoparticles (AgNP) can be applied as bendable and long-term active antimicrobial coatings as shown on the example of PGA-

based surgical sutures (Figure 2). An adapted dip coating technique was developed to equip the investigated surgical sutures in a controlled manner with a silver content of up to $29.7 \mu\text{g}/\text{cm}^2$. The rigid polypeptide polylysine afforded a constant release of silver ions, which is clearly the optimal way of releasing a biocide.

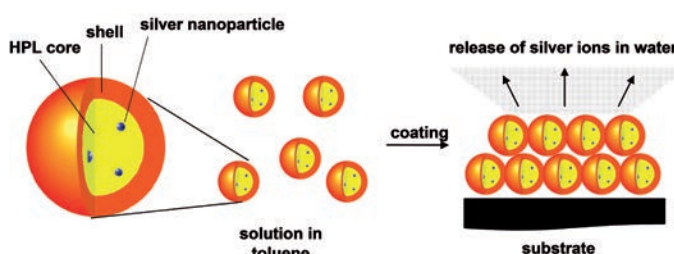


Figure 2: Concept of an antimicrobial coating based of core-shell polylysine nanocontainers with silver nanoparticles.

It could be shown that the release of the silver ions of approx. $0.1 \mu\text{g}$ per cm^2 and day is sufficient to prevent the adhesion of living *S. aureus* cells from their PBS suspension onto the coated sutures. The AgNP loaded sutures FA-HPL are not toxic to mouse fibroblast cells and can be extrapolated to at least 6 weeks of constant silver release showing the maximal antimicrobial effect during this time. Taking into account the typical healing time of wounds, the antimicrobial effect of the coated sutures is sufficient for their practical use.

Thus, polylysine was found to be an easily accessible hyperbranched polymer that can be readily modified to form novel possibly non-toxic core-shell nanostructures for versatile applications. For instance, the AgNP containing coatings with high surface concentrations of AgNPs, form coatings for long-lasting antimicrobial activity and very low cytotoxicity.

Contact:
matthias.thiel@bci.tu-dortmund.de
joerg.tiller@tu-dortmund.de

Publications:

C.H. Ho, M. Thiel, S. Celik, E. Odermatt, I. Berndt, R. Thormann, J. C. Tiller, Conventional and microwave-assisted synthesis of highly branched polylysine towards amphiphilic core-shell nanocontainers for metal nanoparticles, *Polymer* 53 (21), 4623-4630 (2012).

C.H. Ho, E.K. Odermatt, I. Berndt, J. C. Tiller, Long-term active antimicrobial coatings for surgical sutures based on silver nanoparticles and hyperbranched polylysine, *Journal of Biomaterials Science, Polymer Edition* (2013) ASAP.

Biocatalyzed reactions in APCN particles in organic solvents

Overcoming on diffusion limitations

Ina Schönfeld, Stephan Dech, Benjamin Ryabenky, Bastian Daniel, Britta Glowacki, Reinhild Ladisch and Jörg C. Tiller

The use of enzymes as biocatalysts in organic media is an important issue in modern white biotechnology. However, their low activity and stability in those media often limits their full-scale application. Amphiphilic polymer conetworks (APCNs) have been shown to greatly activate entrapped enzymes in organic solvents. However, the biocatalytic conetworks have not yet reached their full potential, because of diffusion limitations. Here, we present a technology to at least partially overcome these limitations and greatly enhance the biocatalytic activity.

In the past, we have shown that amphiphilic polymer conetworks are excellent activating carriers for biocatalysts in organic solvents. Although great activations could be achieved, the reactions were generally diffusion controlled and thus the full potential of these networks was not reached. We investigated the possible increase of the activity of enzymes in different APCNs by preparing microsized particles from these materials. First, we demonstrated this on the example of APCN particles based on PHEA-I-PDMS loaded with α -Chymotrypsin, which resulted in an up to 28000fold higher activity of the enzyme compared to the enzyme powder.

Suspension polymerization and aerosol polymerization were used to synthesize PHEA-I-PDMS microparticles of different compositions in a diameter range of 5 – 80 μm (Figure 1).

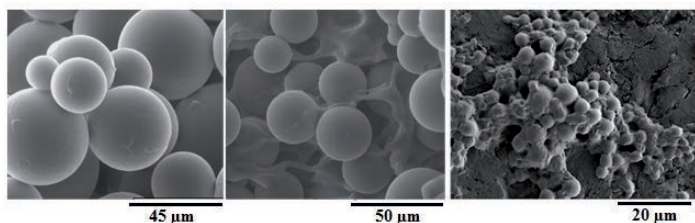


Figure 1: SEM images of PHEA-I-PDMS particles a) prepared by vigorously stirred emulsion polymerization, b) prepared by vigorously stirred emulsion polymerization and subsequent filtration through a 20 μm metal mesh and c) prepared by aerosol polymerization.

The activity of supported α -Chymotrypsin in these microparticles in n-heptane was strongly increasing with decreasing particle diameter. The highest specific activity was 56 U/g for particles with a diameter of 5 μm .

Another particle system consisting of PHEA-I-PEtOx (30/70) in a diameter range of 10 to above 50 μm (Figure 2), loaded with lipase from *Rhizomucor miehei* (RmL) was tested in different organic solvents. In all solvents, smaller particles showed ten to 100fold higher specific activities compared to the native enzyme. This was even true for the production relevant reaction mixture without additional solvent. In the latter case the RmL-loaded PHEA-I-PEtOx microparticles show nearly tenfold carrier activity with some 25-50fold lower enzyme content compared to a commercial product.

Even the smallest particles showed a diffusion limitation of the reaction possibly by surface limited mass

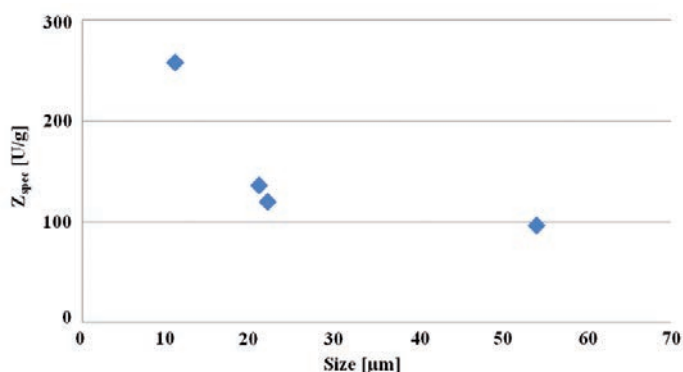


Figure 2: Specific activities (U/g enzyme) of RmL immobilized into PHEA-I-PEtOx (30/70) conetwork particles (RmL content 0.2 wt.%) in correlation to the average particles size (volumetric average). Assay was performed in chloroform

transport, which indicates that the here presented improvement of activity by particularization is still not the highest achievable activation of the APCN supported enzymes. Future investigations are directed towards the application of techniques to further increase the surface/bulk ratio and thus the activity of the biocatalytic APCNs.

Publications:

I. Schönfeld, S. Dech, B. Ryabenky, B. Daniel, B. Glowacki, R. Ladisch, J. C. Tiller, Investigations on diffusion limitations of biocatalyzed reactions in amphiphilic polymer conetworks in organic solvents, *Biotechnology and Bioengineering*, (2013) ASAP.

Contact:

ina.schoenfeld@bci.tu-dortmund.de
joerg.tiller@tu-dortmund.de

Poly(2-oxazoline) based amphiphilic polymer conetworks

How the topology of “near perfect” APCNs effects the properties of such networks

Christian Krumm, Stefan Konieczny, Georg J. Dropalla, Marc Milbradt, Jörg C. Tiller

Defined, controllable and switchable nanostructures are the key features to modern high performance materials. Among them, polymer networks with narrowly size-distributed polymer segments are of great current interest, because they form such regular nanostructures. The regular nanostructure is particularly important for amphiphilic polymer conetworks (APCNs), which contain polymer segments with orthogonal properties, e.g. hydrophilic and hydrophobic behaviour.

Novel APCNs were prepared via end group crosslinking. To this end poly(2-methyloxazoline) (PMOx), poly(2-butyloxazoline) (PBUx) and the triblock copolymers PMOx-*b*-PBUx-*b*-PMOx were prepared by cationic ring-opening polymerization in varying block lengths and telechelically modified with *N,N*-Bis(2-aminoethyl)ethylenediamine (TREN). First the crosslinking with 1,4-dibromo-2-butene (DBB) was established for the homopolymers. The swelling of the obtained materials matches the theoretical value for full crosslinking, indicating that in this way “near perfect” networks could be obtained. Mixtures of the homopolymers and the triblock copolymers were cross-linked with DBB to give APCNs with similar polymer segments but different

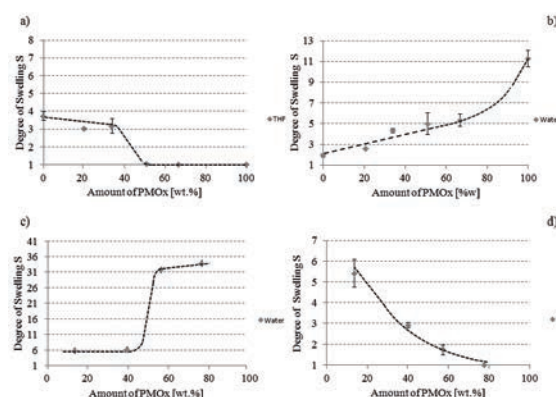


Figure 2: Measurement of the swelling behaviour of differently composed HB-APCN networks in THF (a) and water (b), and of TB-APCNs in water (c) and THF (d).

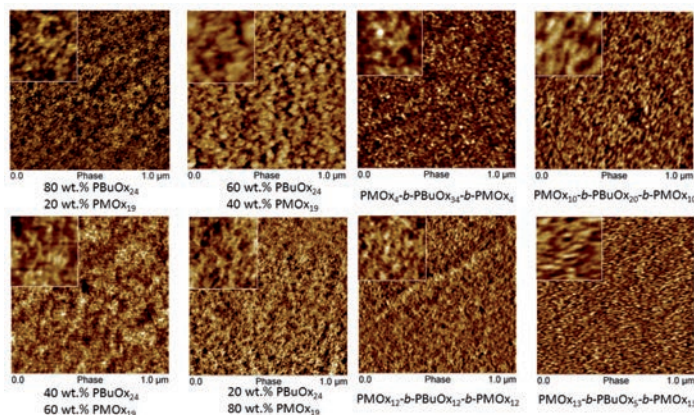


Figure 1: AFM images of homopolymer network mixtures (4 images, left) and of triblock copolymers from PMOx-*b*-PBUx-*b*-PMOx (4 images, right).

network topology.

The nanostructure explored with AFM showed significant differences between mixed homopolymers APCNs (HB-APCNs) (Fig.1 left) and networks derived from ABA triblock copolymers (TB-APCNs). (Fig.1 right) While the first showed areas with typical lamellar structures those are not evident in the TB-APCNs of similar compositions. The more drastic difference between APCNs of different topologies was found in their swelling characteristics, which clearly shows the influence of conetwork structure on their properties.

Contact:
christian.krumm@tu-dortmund.de
joerg.tiller@tu-dortmund.de

Ideally, the nanophases of APCNs, in contrast to common random copolymer networks, should swell independently from the other orthogonal phase in the respective selective solvent. Given the typical nanostructure motives of APCNs this phase should swell only if it is interconnected, which is typically the case around 50% (v/v) and higher. The other phase should act vice versa in presence of its selective solvent. Such a typical behaviour is rarely found for the numerous published APCNs so far. The above described swelling behaviour is found for one phase only (Fig.2). The other phase does not form isolated areas below 50% (v/v). We proposed that this is controlled by the crosslinking strategy. The comparison of the swelling behaviour of HB-APCNs and TB-APCNs clearly supports this thesis. In HB-APCNs the PBUx phase shows the typical APCN behaviour when swollen in THF, while water swells the PMOx phase continuously increasing with greater content. The behaviour is fully inverted in TB-APCNs, which follow a different crosslinking strategy of the two poly (2-oxazoline) phases.

Publications:
C. Krumm, S. Konieczny, G. J. Dropalla, M. Milbradt, J. C. Tiller, *Macromolecules* 46 (9), 3234–3245 (2013).

New Materials for Energy Storage

Mechanical Energy Storage Capacity of Shape Memory Natural Rubber

Benjamin Heuwers, Dominik Quitmann, Frank Katzenberg, Jörg C. Tiller

The storage of energy is one of the greatest current issues. Principally all shape memory materials are able to store mechanical energy due to their capability to memorize a programmed (temporary) shape and recover an original (permanent) shape in the presence of external stimuli. Usually the energy storage capacity of these materials suffers from insufficient reversible deformability and/or retraction force. The previously introduced shape memory natural rubber (SMNR) is a promising candidate for energy storage due to extremely large storable strains of more than 1000%. We found a maximal storable energy of 4.88 J/g for SMNR, which exceeds that of e.g. spring steel (0.13 J/g) by an order of magnitude.

Stored strains of different SMNRs were determined from thermomechanical shape memory cycles. Figure 1 exemplarily shows a shape-memory cycle where the integral $\int F dl$ of the programming path ① corresponds to the energy W_{stretch} needed for stretching the rubber at 50 °C to a strain of 750%. The elastically stored energy W_{stored} during shape recovery at 50 °C is also equal to $\int F dl$ of the recovery path ⑤. Additionally the efficiency η which is the ratio of stored to stretching energy was calculated.

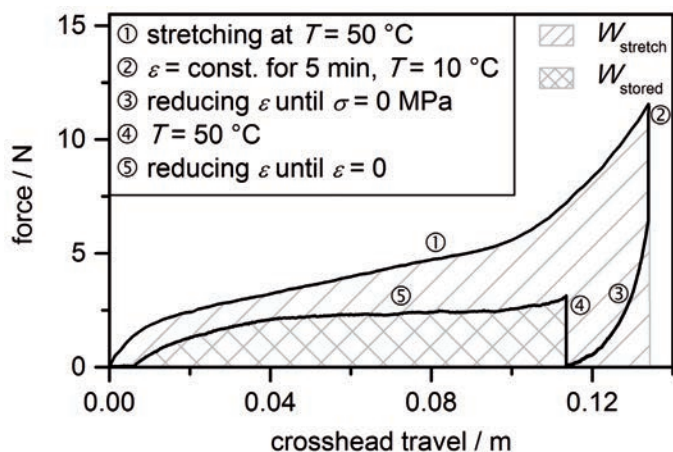


Figure 1: Exemplary plot of force versus crosshead travel of an SMNR sample during a shape-memory cycle.

Values of stored strains for maximally strained SMNRs were obtained in a range from 1.34 to 4.88 J/g with efficiencies η between 26 and 48%. As expected the stored energies increase with increasing degree of cross-linking. The same is true for the efficiencies.

Figure 2 shows the stored energy W_{stored} in dependence on applied strain during programming ϵ_{prog} and degree of cross-linking.

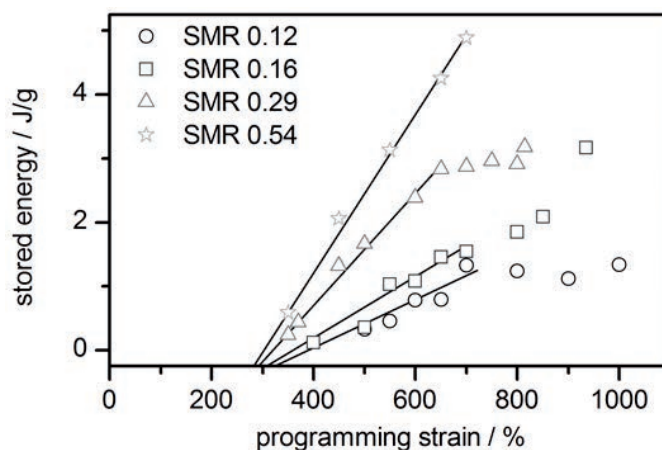


Figure 2: Plot of stored energy W_{stored} against strain during programming ϵ_{prog} for differently crosslinked SMNRs. The names of samples refer to their degrees of cross-linking (determined by mechanical measurements).

Interestingly, starting from low elongations the stored energy W_{stored} increases linearly with programming strain ϵ_{prog} and all lines intersect at some 300%. Obviously, it is not possible to store energy by the shape memory effect in SMNR below 300% under the given conditions. Particularly the lower cross-linked samples that store less energy show a deviation of the linear trend at higher strain.

The here reported stored energy values are by an order of magnitude higher than previously reported for other SMPs.

Publications:

B. Heuwers, A. Beckel, A. Krieger, F. Katzenberg, J. C. Tiller, *Macromolecular Chemistry and Physics* 2013.

B. Heuwers, D. Quitmann, R. Hoehner, F. M. Reinders, S. Tiemeyer, C. Sternemann, M. Tolan, F. Katzenberg, J. C. Tiller, *Macromolecular Rapid Communications* 2013, 34, 180-184.

Contact:

benjamin.heuwers@tu-dortmund.de
 dominik.quitmann@tu-dortmund.de
 frank.katzenberg@tu-dortmund.de
 joerg.tiller@tu-dortmund.de

Extending the Limits of Shape Memory Polymers

World Record in Strain Storage

Robin Höher, Frank Katzenberg, Jörg C. Tiller

Shape memory polymers (SMPs) are an important class of smart materials. However, the potential of these macromolecular networks regarding their storable strain was not maxed out. In order to enhance the strain storage capacity of SMPs we prepare polymer networks with a degree of cross-linking at the borderline between thermoplastics and elastomers. By applying this concept to different polyethylenes we obtained SMPs that are capable to store strains up to 1409%. All investigated polymers show higher strain storage than literature reported systems and exhibit excellent shape memory parameters.

The goal of this study was the enhancement of the strain storage capacity of shape memory polyethylene. For this study we choose high density polyethylene (HDPE), low density polyethylene (LDPE) and ethylene-1-octene copolymer (EOC) as commercially available polyethylenes and dicumyl peroxide as cross-linking agent. In order to explore if the products are at the borderline between thermoplastics and elastomers, networks with varying DCP concentration were prepared. The DCP concentration to achieve the critical degree of cross-linking was assumed to be obtained when the Young's modulus remains constant above the melting temperature within the measured temperature range. For HDPE we found a critical DCP concentration of 0.2 wt.-%. For LDPE and EOC the critical concentration was determined to 0.3 and 0.5 wt.-%. For these critically cross-linked networks the strain storage capacity was determined.

The major parameter for high strain storage is the maximally achievable strain ϵ_{\max} , which was obtained to 1070% for HDPE/0.2, 1200% for LDPE/0.3 and 3000% for EOC/0.5. Thus we were able to exceed the so far reported ϵ_{\max} of 800% by a factor of more than three.

Further typical criteria for high strain storage are the recovery as well as fixity ratios. The recovery ratio R_r describes the degree of plastic deformation after each shape memory cycle, whereas the fixity ratio R_f characterizes how much of the applied maximum strain can be stabilized in the temporary shape. Hereby a preferably high recovery as well as fixity ratio is aspired. In order to determine the recovery and fixity ratios of the polyethylene samples, cyclic mechanical measurements were carried out over ten cycles. All three polyethylene networks show high recovery ratios of 98–100% and therefore only small permanent plastic deformation. The fixity ratios were obtained to 100% for HDPE/0.2, 99% for LDPE/0.3 and 87% for EOC/0.5 and correlate to the degree of crystallinity, which decreases with increasing content of branching.

The stored strains ϵ_{stored} were calculated to 1061% for HDPE, 1180% for LDPE and 2440% for EOC within the first and to 875%, 957% and 1409% after the tenth cycle, respectively. As shown in Figure 1, the strain storage capacity of EOC-SMPs clearly exceeds that of conventional PE-SMPs.

We found the highest potential to store large strains for

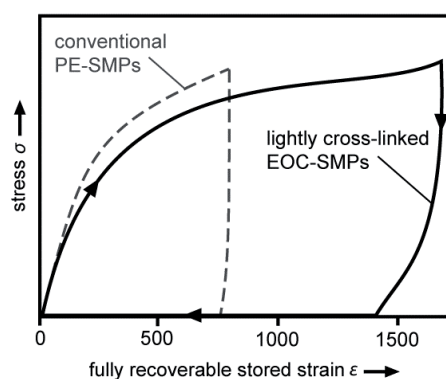


Figure 1: Illustration of the strain storage capacity of conventional PE-SMPs and lightly cross-linked EOC-SMP.

networks of ethylene-1-octene copolymer (EOC) with a fully recoverable stored strain of about 1400% after three conditioning cycles. This is by far the largest reported stored strain value of shape memory polymers.

Contact:

robin.hoeher@tu-dortmund.de
frank.katzenberg@tu-dortmund.de
joerg.tiller@tu-dortmund.de

Publications:
R. Hoeher, T. Raidt, M. Rose, F. Katzenberg, J. C. Tiller,
Journal of Polymer Science Part B: Polymer Physics 51 (31),
1033-1040 (2013).



Chemical Biotechnology (BT)

Biocatalytic gram-scale production of (S)-limonene

Harnessing an orthogonal genetic pathway for monoterpene formation from cheap and renewable resources in metabolically engineered *Escherichia coli*

Christian Willrodt, Christian David, Bruno Bühler, Mattijs K. Julsing, Andreas Schmid

The use of a metabolically engineered *E. coli* strain containing an orthogonal biosynthetic pathway for monoterpenoids allowed the gram-scale production of (S)-limonene from renewable glycerol. Limonene concentrations up to 2.8 g L⁻¹ and maximal productivities of 40 mg L⁻¹ h⁻¹ were achieved with an in situ product removal system, which additionally facilitated the product purification by vacuum distillation. This study reports the highest productivity and titer for fermentative production of a monoterpene in a microbial host so far.

Throughout the past decade extensive research has been conducted to improve microbial platform organisms for the production of industrially and pharmacologically relevant terpenoids. However, engineering of microbes almost exclusively focused on the biosynthesis of sesqui-, di-, and tetra-terpenes. The production of monoterpene structures in *Escherichia coli* and *Saccharomyces cerevisiae* has been investigated to a lower extent, although numerous high-value products can be found among them and their derivatives.

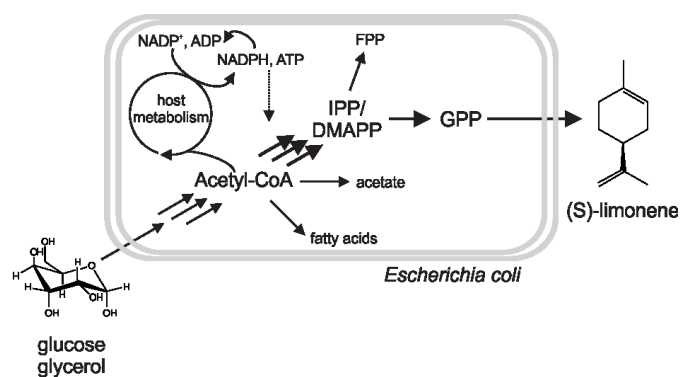


Figure 1: Schematic overview of the fermentative production of (S)-limonene from renewable resources like glucose or glycerol with its dependency on host intrinsic metabolism, energy supply, and cofactor regeneration.

This study reports the first productive approach toward the fermentative synthesis of monoterpenes from glucose or glycerol (Fig. 1). As model compound, (S)-limonene was selected, an industrially relevant chiral molecule. The carbon source is converted by the host metabolism to acetyl coenzyme A, which serves as the starting compound for terpenoid biosynthesis. Supply of sufficient amounts of the terpenoid precursors IPP and DMAPP is guaranteed by the incorporation of the foreign mevalonate pathway [1]. Two additional enzymes from plant origin are used to form (S)-limonene. GPP is the direct precursor for all monoterpenes and thus, this system can be easily adapted for the synthesis of other monoterpenes by exchanging the gene coding for limonene synthase.

Contact:

christian.willrodt@bci.tu-dortmund.de
mattijs.julsing@bci.tu-dortmund.de
andreas.schmid@bci.tu-dortmund.de

The recombinant *E. coli* strain produced (S)-limonene at a final titer of ~2.8 g L_{org}⁻¹ in a 45 h, glycerol limited, 2-liquid phase fed-batch cultivation (Fig. 2). The maximum productivity during this cultivation was 40 mg L⁻¹ h⁻¹, which approached already the requirements for production processes for fine chemicals, although minor effort was put in reaction and process optimization up to this point [2]. (S)-limonene was recovered from the fermentation broth by vacuum distillation with a purity of ≥ 96% (e.e. ≥ 99.8). Future work will aim at both, strain and reaction engineering in order to optimize the syntheses of monoterpenes and derivatives from renewable feedstocks.

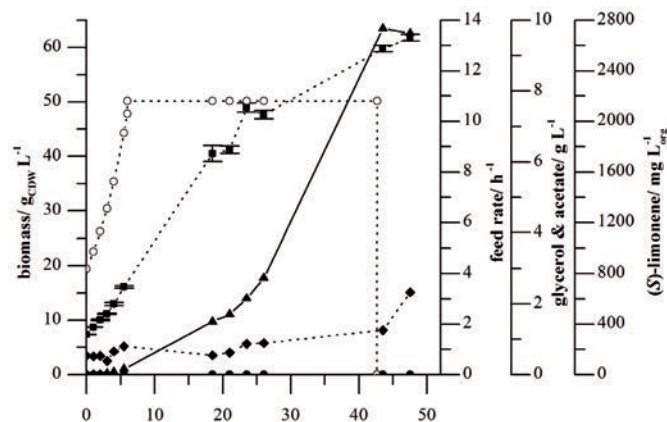


Figure 2: Fermentative production of (S)-limonene during a glycerol limited fed-batch cultivation of *E. coli* BL21 (DE3) harboring the heterologous limonene formation pathway. Diisononyl phthalate (0.5 L) was added as organic phase (total volume 1.5 L). Concentrations of biomass (■), glycerol (●), acetate (◆), limonene (▲) as well as the glycerol feed rate (○) are given.

References: [1] Martin *et al.*, 2003, *Nat. Biotechnol.* 21(7):796-802.

[2] Schrewe *et al.*, 2013, *Chem. Soc. Rev.* (published online) DOI: 10.1039/C3CS60011D

Publications:

C. Willrodt, C. David, S. Cornelissen, B. Bühler, M. K. Julsing, A. Schmid, manuscript in preparation

Poster: Monoterpene Production in Metabolically Engineered *Escherichia coli*, C. Willrodt, B. Bühler, M. K. Julsing, A. Schmid, BioCat Conference 2012, Hamburg, Germany.

Characterization of a proline-hydroxylating whole-cell biocatalyst

An insight on the interrelationship between catalytic activity and cell physiology

Francesco Falcioni, Oliver Frick, Lars Blank, Bruno Bühler, Andreas Schmid

Proline addition to a minimal medium and codon optimization was found to significantly enhance production of the recombinant protein proline-4-hydroxylase (P4H) in recombinant E. coli. Comparison of mRNA levels revealed that, while proline addition affects P4H synthesis at the translational level, codon optimization greatly influenced mRNA stability. Comparison with in vitro activities confirmed that the available P4H activity was not fully exploited in whole cells and that the current limitation of the biocatalytic activity comes from host metabolism.

In this study we investigated the catalytic activity of recombinant *Escherichia coli* expressing a gene for proline-4-hydroxylase (P4H). P4H, a 2-ketoacid-dependent non-heme iron dioxygenase, catalyzes the hydroxylation of proline with O₂ as oxygen donor. The second oxygen atom of O₂ flows into the oxidative decarboxylation of 2-oxoglutarate to succinate and CO₂. Its strong interconnection with cellular metabolism makes P4H an ideal system to study the interrelationship between biocatalysis and cell physiology.

Specific proline hydroxylation activities of cells grown in minimal medium on glucose were found to be low. It was hypothesized that P4H synthesis may be limited by proline depletion as a consequence of the P4H activity. Indeed, addition of proline (either pure or in yeast extract) had a positive impact on both P4H synthesis and activity.

It was speculated that proline availability affected P4H synthesis via the pool of charged prolyl-tRNAs. To test this hypothesis, an alternative codon optimization approach was tested in which all non-rare host codons were used in the recombinant gene (*p4h1of* gene). In the original approach, only the most abundant host-codon had been used (*p4h1or* gene). The new gene indeed resulted in much higher P4H levels. This effect was cumulative with that of proline (Fig. 1).

Analysis of *p4h1or* and *p4h1of* mRNA levels revealed that the presence of proline did not modify mRNA levels of either gene, confirming that the beneficial effect of proline on P4H synthesis occurs at the translational level.

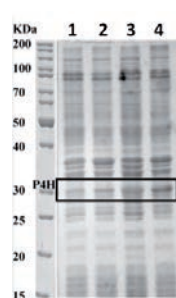


Figure 1: Soluble P4H levels in cell extracts from cultures of *E. coli* BL21 (DE3) (pLysS) carrying either pET_p4h1or (with the *p4h1or* gene) or pET_p4h1of (with the *p4h1of* gene). Cells were cultivated at 30°C and harvested 4 h after induction by IPTG. Lane 1, *E. coli* BL21 (DE3) (pLysS) (pET_p4h1or) grown on glucose only; Lane 2, same strain grown on glucose and proline; Lane 3, *E. coli* BL21 (DE3) (pLysS) (pET_p4h1of) grown on glucose only; Lane 4, same strain grown on glucose and proline.

In contrast, mRNA levels of *p4h1of* were ~10-fold higher than those of *p4h1or*, suggesting that codon optimization influenced mRNA stability. However, specific resting cell activities did not correlate with the different P4H levels (Fig. 1), but rather a maximum activity was reached at 6-6.5 U/g_{CDW} in three of the four cases (Fig. 2a). In comparison, P4H activities of permeabilized cells provided with the cosubstrate 2-oxoglutarate were higher (Fig. 2b) and correlated well with the soluble P4H levels (Fig. 1) showing that the P4H activity available in the whole-cell biocatalyst is not fully exploited.

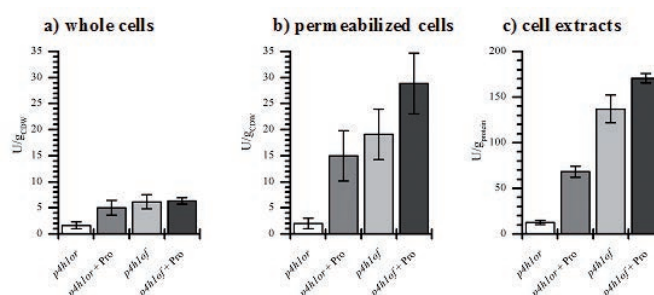


Figure 2: Activities for strains and conditions corresponding to those described in the legend of Fig. 1. (a) resting cell activities. (b) activities of permeabilized cells. (c) cell extract activities. 1U = 1 μmol product/min.

These results clearly emphasize the dependency of whole-cell biocatalyst performance on host physiology, which thus must be considered for biocatalyst and process engineering.

Publications:

F. Falcioni, L. M. Blank, O. Frick, B. Bühler, A. Schmid, Proline availability regulates proline-4-hydroxylase synthesis and substrate uptake in proline-hydroxylating recombinant *E. coli*. (2013) *Appl. Environ. Microbiol.* 79(9):79-87.

Contact:

francesco.falcioni@bci.tu-dortmund.de
bruno.buehler@bci.tu-dortmund.de
andreas.schmid@bci.tu-dortmund.de

A new chassis for industrial biotechnology: *Pseudomonas taiwanensis* VLB120

In-depth taxonomic analysis of *Pseudomonas taiwanensis* VLB120

Kirsten A.K. Köhler, Lars M. Blank, Birgitta E. Ebert, Christian Rückert, Jörn Kalinowski, Andreas Schmid

A combination of comparative genomics with traditional taxonomic methods characterized the organism *Pseudomonas taiwanensis* VLB120 as the only known non-pathogenic solvent-tolerant *Pseudomonas* strain known so far. In these studies a comprehensive method to reveal the taxonomy of the solvent-tolerant *Pseudomonas* strain was applied including 16S rRNA, housekeeping genes and full genome comparisons, as well as physiological data including carbon and nitrogen source usage and cell membrane composition. During the course of the study currently applied taxonomic methods were regarded critically to answer the question, which of these tools are suitable for the taxonomic identification and classification of *Pseudomonas* species.

The genomic inventory of *P. taiwanensis* VLB120, consisting of a 5.6 Mbp genome and the 320 kbp megaplasmid pSTY was investigated. The genomic inventory of this strain compares well to other solvent-tolerant *Pseudomonades*, all known as potentially opportunistic pathogens, but also to non-pathogenic *Pseudomonas* strains. In a genome wide comparison of genes described as potential virulence factors of opportunistic pathogenic and other non-pathogenic members of the genus *Pseudomonas* with the isolate, it clustered with the non-pathogenic species, supporting that *P. taiwanensis* VLB120 is indeed a non-pathogenic member of the genus *Pseudomonas*. With the genomic information in hand, it was aimed for the taxonomic classification of the strain, which was intriguingly indistinct, depending on the methods used. Therefore a comprehensive approach on the investigation of *Pseudomonas* taxonomy including 16S rRNA, housekeeping genes and full genome comparisons as well as physiological data was applied. The analyses of all these data indicated that the isolate is a member of the species *P. taiwanensis* (Fig. 1). It was also observed, that the *P. putida* type strain does not cluster with other *P. putida* strains when comparing 16S rRNA - which was also reported in the literature - while in a whole genome comparison and the comparison of housekeeping genes it does, underlining the complexity of classifying *Pseudomonas* strains. This contrast clearly shows that a classification of *Pseudomonades* is only possible by integrating all available sequence and physiological data.

The major difference of the isolate to the *P. taiwanensis* type strain is its ability to develop a solvent-tolerant phenotype. To compare the solvent tolerance behavior of the two strains, both strains were cultivated in LB medium adding toluene or styrene to the culture medium.

The *P. taiwanensis* type strain was not able to grow in either the presence of styrene or toluene, while *P. taiwanensis* VLB120 was able to grow in the presence of both solvents after a short lag phase (Fig. 2).

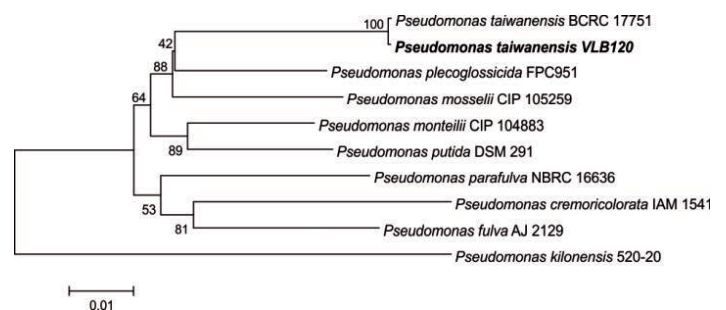


Figure 1: Neighbor joining tree based on the concatenated sequences for 16S rRNA and the housekeeping genes *gyrB*, *rpoB*, *rpoD* of *P. taiwanensis* VLB120 and *Pseudomonas* type strains. The percentage of replicate trees that were found by Bootstrap testing (500 replicates) is shown next to the branches.

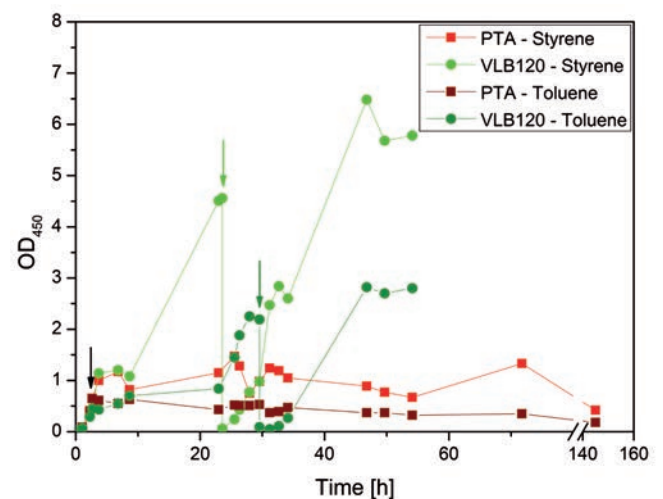


Figure 2: Organic solvent tolerance test of *P. taiwanensis* VLB120 (VLB120) and *P. taiwanensis* type strain (PTA). The addition of 1 % styrene or toluene was performed at an OD_{450} of 0.5 – 1 (first arrow). Cells that showed growth behavior in the presence of styrene and toluene were then transferred into fresh medium, directly containing 1 % of the respective solvent (second arrow) to show the adaptation of the cells.

Publications:
K. A. K. Köhler, L. M. Blank, B. E. Ebert, C. Rückert, J. Kalinowski and A. Schmid; In depth genomic analyses reveal a new chassis for industrial biotechnology: *Pseudomonas taiwanensis* VLB120; in preparation.



Biochemical Engineering (BVT)

Immobilization of tyrosinase in alginate matrix capsules

Entrapment of whole cells from *Agaricus bisporus* for removal of phenolic compounds

Markus Kampmann, Rolf Wichmann

The detection of endocrine disrupting phenols in waste and surface waters has received considerable attention. The enzymatic oxidation with tyrosinase and subsequent removal of the formed quinones has been suggested as a treatment method. We used the edible mushroom Agaricus bisporus as enzyme source and were able to disintegrate the mycelium and to immobilize tyrosinase containing cells, what might be useful to significantly reduce the enzyme costs.

Biocatalysts are usually immobilized in order to protect them against deactivation and to facilitate their handling, separation and reutilisation. One option is the entrapment in alginate matrix capsules. Some advantages are the high biocompatibility and mild immobilization methods. However, when applied to immobilization of tyrosinase, leaching of enzyme from the alginate capsules is a fundamental challenge. Additionally, with respect to an application, e.g. wastewater treatment, the enzyme costs have to be minimized.

By a targeted modification of the capsule material, i.e. combination of different polymers and additives, and evaluating enzyme loading, we were able to reduce tyrosinase leaching from alginate capsules and increase enzyme activity to a significant extent.

In order to further reduce enzyme leaching and to save enzyme costs, we investigated the immobilization of tyrosinase containing cells from the edible mushroom *A. bisporus* instead of isolated tyrosinase.

For this purpose, we have established an experimental procedure to disintegrate the mycelium of *A. bisporus* (Figure 1). After disintegration the cells and cell debris were entrapped in alginate matrix capsules and still showed tyrosinase activity. Moreover the immobilized biocatalysts maintained tyrosinase activity for a longer period of time as compared with the native biocatalysts under same storage conditions (Figure 2).

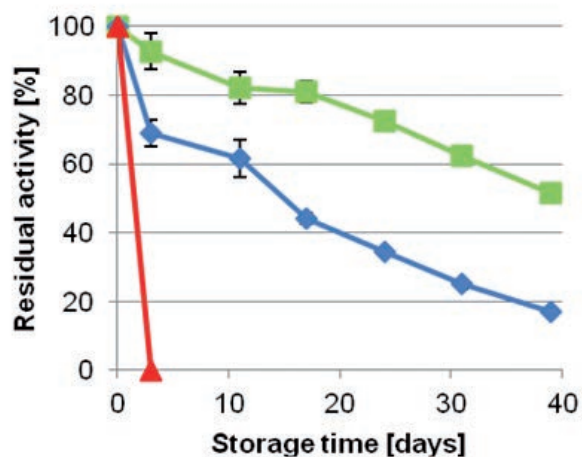


Figure 2: Stability of tyrosinase in *A. bisporus* stored in H₂O at room temperature: cell suspension (red), cells immobilized in alginate (blue) and in silica alginate (green) matrix capsules.

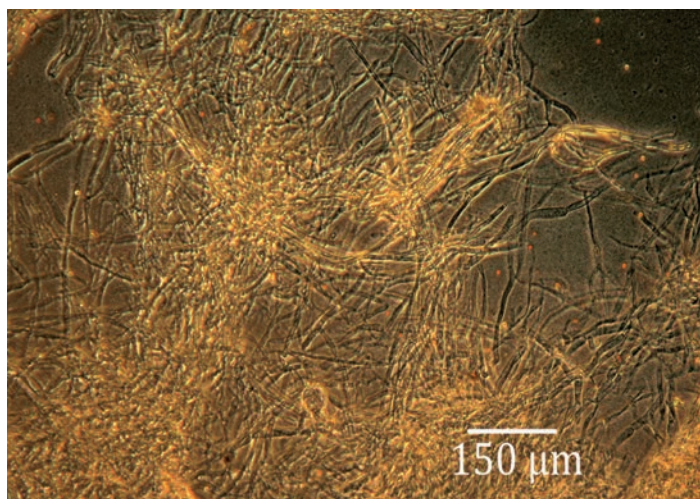


Figure 1: Mycelium from *A. bisporus*.

The generated catalyst systems were also capable to oxidize endocrine disrupting bisphenol A and therefore might be useful for wastewater treatment.

This will be further investigated by application of the immobilized catalysts to operate in continuous mode and development of a kinetic model for the tyrosinase catalyzed oxidation of bisphenol A.

Contact:
markus.kampmann@bci.tu-dortmund.de
rolf.wichmann@bci.tu-dortmund.de

Publications:
Kampmann, M., Kleiner, B., Breden, M., Bielecki, J., del Amor Villa, E.M., Wichmann, R., Improving the immobilization efficiency of enzyme in alginate microcapsules, Poster presentation, Third CLIB Graduate Cluster Annual Retreat, Bergisch Gladbach, Germany (2012).
Kampmann, M., Kleiner, B., Bielecki, J., Uhl, S., Wichmann, R., Biopolymer-Immobilisierung von Tyrosinase zur Entfernung von Bisphenol A, Oral presentation, ProcessNet-Jahrestagung und 30. Dechema Jahrestagung der Biotechnologen, Karlsruhe, Germany (2012).

Scale-Up of the production of Biosurfactants

Production and isolation of monorhamnolipids produced by *Pseudomonas putida*

Benjamin Küpper, Lisa Halka, Adam Imhoff, Anika Mause, Christian Nowacki, Rolf Wichmann

Biosurfactants like rhamnolipids have the potential to replace or support synthetic surfactants based on crude oil in the long run due to their antimicrobial properties and biodegradability. The main disadvantage is that monorhamnolipids currently are not commercially available. As a part of this project, which is funded by the Deutsche Bundesstiftung Umwelt (DBU 13235/02), one goal is the production of sample material for project partners to obtain more information about the performance and the applicability of the target substances. The other goals are the implementation of an economically feasible fermentation process as well as the establishment of a downstream process that uses environmental friendly substances and is easy to use.

The production of rhamnolipids at a larger scale is primarily established by using bacteria of the pathogenic species *Pseudomonas aeruginosa* and with plant oils as substrates which increases the costs for process safety and the following downstream processing because costly operations like for example liquid-liquid extraction have to be used. Instead, *Pseudomonas putida* as a well-known host organism for genetic modifications can be cultivated under S1 conditions easily and glucose as the only carbon source does not affect the implemented capture step via hydrophobic adsorption.

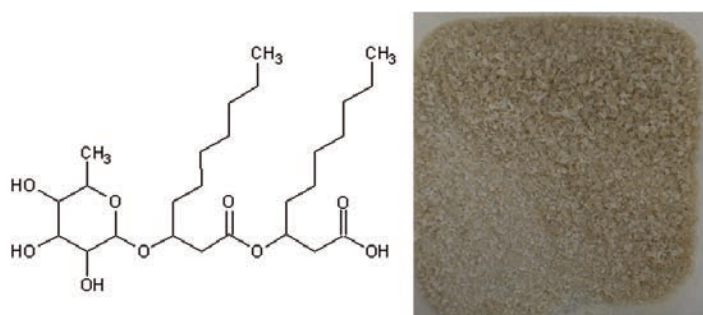


Figure 1: Monorhamnolipid molecule (left) and produced sample substance for application tests (right).

The first challenge in the production of rhamnolipids in a stirred and aerated fermentor is the excessive foaming. This leads to termination of the fermentation process after a few hours due to depletion of the cells in the fermentation medium by foaming out with the exhaust air. The cell-containing foam also blocks the ceramic exhaust air filters. To be able to extend the time for the

rhamnolipid production, no mechanical foam destroyer is used and no chemical defoamers can be used at high rhamnolipids concentrations, but instead the foam is led out of the fermentor through a tube and collected in a container where it can be separated from the exhaust air and rest to collapse. After separation of the cells from the broth or the collapsed foam, an adsorption step follows. The aqueous phase is pumped through a column filled with a hydrophobic adsorbent to utilize the amphiphilic properties of the rhamnolipids which leads to its adsorption. A washing step with water removes the hydrophilic components like glucose or other substrates. After desorption with ethanol/water mixtures, the fractions containing rhamnolipids are freeze-dried to a slightly yellowish-white powder (Fig.1). Earlier adsorption/desorption experiments lead to a brownish-orange product with a low purity if the desorption process was carried out using pure ethanol without separation of the eluted fractions. A red/yellowish pigment produced in the fermentation process can be removed by controlled elution (Fig. 2).

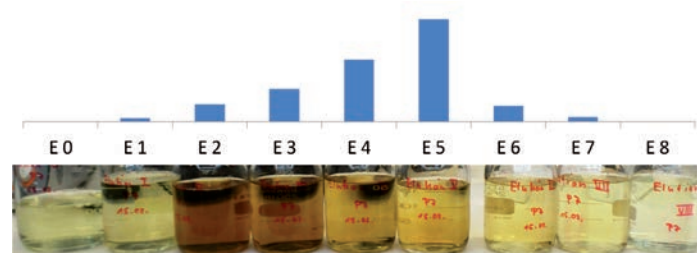


Figure 2: Elution fractions after desorption with rhamno-lipid content given above.

Publications:

Oral presentation at ProcessNet 2012, Karlsruhe:
„Fermentative Herstellung und Aufarbeitung von Monorhamnolipiden“.
Oral presentation at Biosurfactants - Challenges and Perspectives 2013, Frankfurt am Main: „Fermentative Production and Downstreaming of Monorhamnolipids“.
Küpper B, Halka L, Imhoff A, Mause A, Nowacki C, Wichmann R;
„Fermentative Produktion von Monorhamnolipiden im Pilotmaßstab – Herausforderungen der Maßstabsvergrößerung“, DOI: 10.1002/cite.201200194 in der Chemie Ingenieur Technik Volume 85, Issue 6, pages 834–840, June, 2013.

Contact:

benjamin.kuepper@bci.tu-dortmund.de
christian.nowacki@bci.tu-dortmund.de
rolf.wichmann@bci.tu-dortmund.de



Chemical Reaction Engineering (CVT)

Energy-efficient adsorptive CO₂-capture from cement flue gas

Optimised CO₂-adsorption with amine-functionalised adsorbent and phase change materials

Jan Frederik Horstmeier, David W. Agar

Non-energy related CO₂ generation, e.g. from cement and steel manufacture, is considerable and effectively unavoidable. Such plants often operate within an entirely different framework to power stations. It is thus necessary to reassess the suitability of the prevailing absorptive alkanolamine scrubbing technology for these cases, especially in view of unresolved issues such as chemical degradation, the high energy demand for solvent regeneration and corrosivity.

Adsorption process, and in particular, vacuum swing adsorption (VSA), offer a promising alternative to CO₂ capture by liquid alkanolamine solvents.

Amine-functionalised adsorbents can yield higher capacities and selectivities in CO₂ adsorption process, albeit at the cost of a higher heat of adsorption, due to the stronger chemical bonding.

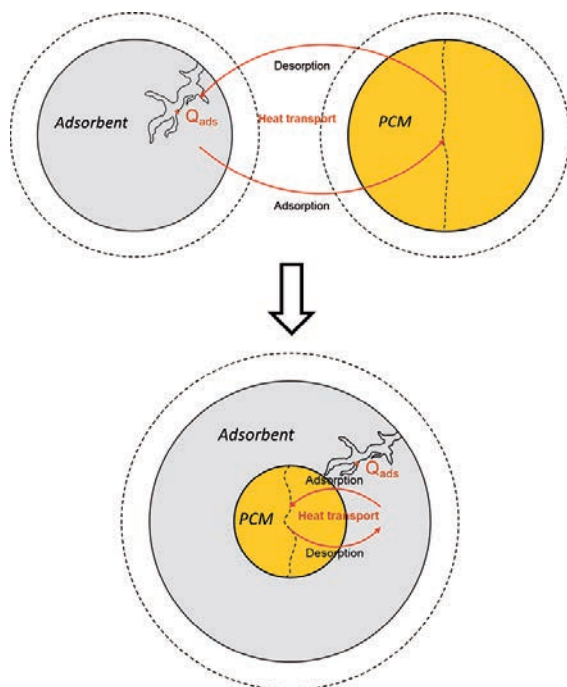


Figure 1: Different strategies to integrate the PCM for optimal exploitation (Homogenous Bed ↔ Combined Particle).

To ameliorate this problem, Phase Change Material (PCM) can be incorporated into the adsorbent fixed bed, which take up the heat liberated in the exothermic adsorption phase through a liquefaction phase change at a prespecified temperature. During the desorption step this heat is then released for the regeneration of the adsorbent. (Fig.1)

The integration of PCM thus decreases the temperature variations and renders the whole process more efficient, both by increasing the CO₂-capacity and decreasing the overall energy demand. The increase of efficiency depends on the integration technique, because of the different dominating heat transport resistances in the homogenous bed and the combined particle. (Fig. 2)

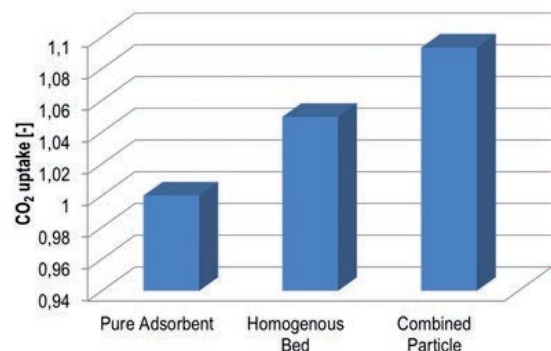


Figure 2: Standardised CO₂ uptake for different PCM insertion.

Modelling and simulation of the entire cyclic adsorption process with its individual steps has been carried out to optimise the design, operating conditions and PCM integration.

Experimental research on the optimal preparation of Amine-functionalised adsorbents, their adsorption characteristics and the use of PCMs in the packed bed is also being carried out.

Publications:
Horstmeier, J. F., Heib, S., Herrmann, J., Keseberg, D., Agar, D. W., „Prozessinterne Rückgewinnung der Adsorptionswärme zur effizienten CO₂-Adsorption aus Industrieabgasen“, DECHEMA Process-Net Jahrestreffen Fachgruppe Adsorption 2013.

Contact:

jan-frederik.horstmeier@bci.tu-dortmund.de
agar@bci.tu-dortmund.de

Capillary microreaction engineering

Suspension catalysis in liquid-liquid microreactors

Frederik Scheiff, David W. Agar

Suspension catalysis in liquid-liquid slug flow is a potential alternative for micro-fixed-bed or catalytically coated wall microreactors, but seldom the subject of microreaction engineering research. The particle dynamic effects of the complex three-phase flow have been investigated.

The so-called slug flow, a segmented flow of two immiscible liquids in microcapillaries, offers advantages such as precisely defined residence times and an enhanced mass transfer within and between the two phases. The latter is governed by Taylor-like vortices, which promote the interplay of convective and diffusive transport in each slug. However, these effects have not yet been exploited for heterogeneous catalysis. Instead, heterogeneous reaction concepts in microreactors have been restricted to either micro-fixed-beds or catalytically coated wall reactors. Nevertheless, the suspension catalysis in particular can provide clear benefits in terms of catalyst accessibility for both reactants and its recovery by virtue of its wetting properties, as long as the particles remain well accessible.

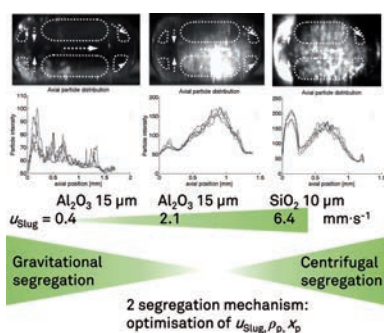


Figure 1: Local particle distribution (fluorescent-optical image analysis as a function of x_p , D_p , u_{slug} , particle load, residence time within paraffin oil – H₂O flow (overlay of 5 individual slug snapshots)).

Fig. 1 shows hydrophilic particles suspended in the disperse, aqueous phase (surrounded by an organic phase), which is the most frequent case referring to the use of mostly hydrophilic catalyst materials like Al₂O₃ or SiO₂. And for these typical catalyst supports segregation in an almost stagnant rear subvortex has

been verified experimentally by means of fluorescent-optical resolution of the local particle distribution. The accumulation in the nearly quiescent region has been found to decelerate liquid-solid mass transfer and is undesired, accordingly.

It has therefore been the scope of our research to decipher the fluiddynamic source of the segregation and to establish countermeasures on this basis. The forces acting on a single microparticle have been obtained experimentally by fluorescent particle tracking (PTV) and estimated theoretically based on simplifying assumption on the flow (Fig. 2, gray areas). One example of these forces as a function of particle diameter is shown in Fig. 2. Besides the good agreement between experimental and theoretical analysis, these results provide novel insight into the particle motion. Until now, the comprehension of particle segregation is limited to gravitational settling at low flow rates. However, the results in Fig. 1 and 2 provide evidence for a second mechanism - the centrifugal segregation - with a crucial consequence: The rate of suitable flow rates is not only limited by a minimum threshold for gravitational settling, but also by a maximum threshold for centrifugal segregation.

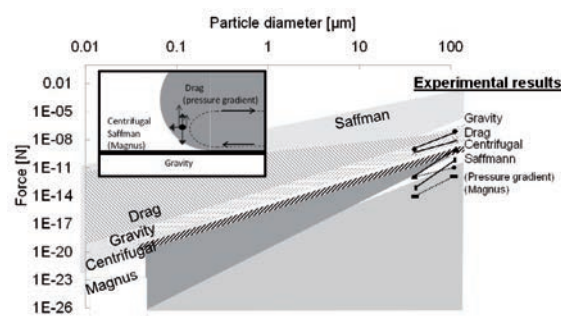


Figure 2: Experimental & theoretical evaluation of forces on microparticles: calculated from microscopical fluorescent particle tracking (Al₂O₃ catalyst particles in H₂O - paraffin oil slug flow, $u_{\text{slug}} = 0.123$ m·s⁻¹).

After all, this piece of research extends the knowledge on microparticle motion in slug flow and optimization of the suspension slug flow microcapillary reactor by fluid dynamic means.

Contact:
 frederik.scheiff@bci.tu-dortmund.de
 agar@bci.tu-dortmund.de

Publications:

Scheiff, F., Agar, D. W. Suspension slug flow microreactor – an innovative concept for heterogeneous catalyzed reactions, Poster presented at “Jahrestreffen Hochtemperaturtechnik und Technische Reaktoren”, 26 - 27.02.2013, Oberhausen, Germany.



Process Dynamics and Operations (DYN)

Monitoring emulsion polymerisations by ultra-sound velocity

A possible contribution to sensor fusion for robust observation of polymerisations

Heiko Brandt, Sebastian Engell

As often shown in the literature and also demonstrated in industrial applications [1], model-based control techniques are suitable to reduce batch times in polymer production. Reducing the batch time is achieved by feeding the ingredients as fast as possible while still producing a polymer that has desired properties. The successful application of such control solutions requires an estimation of the inner states of the process, in particular of the hold-ups of the different monomers. For homopolymerisations with sufficient heat of reaction, this estimation is possible using temperature measurements, but for copolymerisations, the estimation is no longer robust. Therefore additional concentration-dependent measurements that can be implemented in industrial practice are of great interest. In this study we examined the potential of ultra-sound velocity measurements for monitoring the reaction progress in emulsion polymerisations.

The process of emulsion polymerisation uses the basic ingredients water, emulsifier, initiator and monomer. Depending on the recipe, up to three different phases are present in the reactor, a matrix phase mostly containing water, a droplet phase mostly containing monomer, and a micelle/particle phase which is stabilized by the emulsifier in which the polymerisation reaction mainly takes place (Fig. 1).

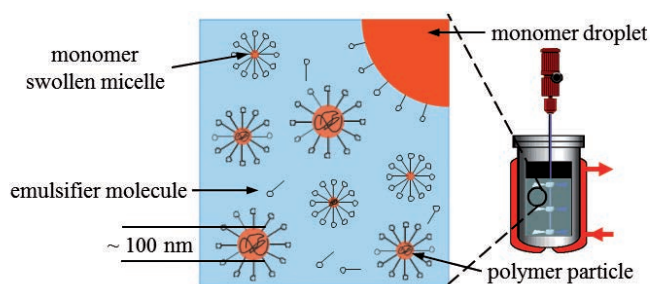


Figure 1: The complex nature of an emulsion polymerisation process.

(Ultra)-sound velocity (SV) is a property of chemical mixtures that can easily be determined by measuring the time a pulse of sound needs to cover a certain distance across the fluid.

As time can be measured with high resolution, the sound velocity can be determined with high accuracy and reproducibility. Furthermore the available sensors are cheap and mature.

To relate the sound velocity to the concentrations of the species, the model developed by Siani [2] is used. The model employs the densities and the adiabatic compressibilities of the pure substances and contains four adjustable parameters to account for mixing nonlinearities. If a model of the sound velocity as a function of the concentrations is available, the measurements can be integrated into the estimation of the hold-ups by a so-called observer.

In order to investigate the applicability of the sound velocity measurement to monitor emulsion polymerizations,

styrene homopolymerisations were considered. It turned out that an individual fit is possible for all recipes and the models predict the sound velocity well. Fig. 2 shows a validation experiment where parameters from other experiments were used. Two experiments are reproduced excellently while the third is not matched well, probably because of significantly different chain lengths of the polymer.

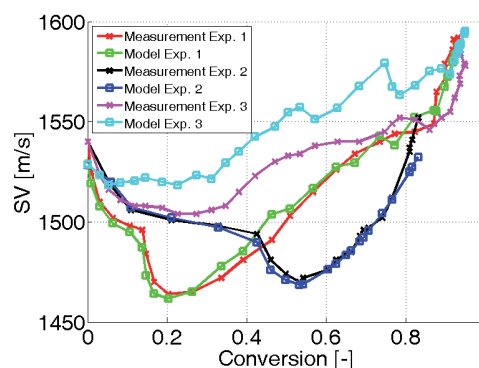


Figure 2: Conversion data versus measured and simulated values of sound velocity for different styrene emulsion polymerisations.

Our conclusion is that process monitoring using ultra-sound velocity is possible, but that the range of validity of a certain set of parameters is limited to similar recipes or products. Thus it is suitable to be integrated into state estimation for operating conditions around a nominal batch trajectory.

[1] T. Finkler, M. Kawohl, U. Piechottka, S. Engell, IFAC Proc., 11-18, 2012

[2] A. Siani, G. Storti, M. Morbidelli, J. Appl. Polym. Sci., 72, 1451-1477, 1999

Publications:

H. Brandt, D. Sühling, S. Engell, Monitoring Emulsion Polymerization Processes by Means of Ultra-Sound Velocity Measurements, Conference: 12th AIChE Annual Meeting, 2012.

Contact:

heiko.brandt@bci.tu-dortmund.de
s.engell@bci.tu-dortmund.de



Fluid Separations (FVT)

Process intensification for CO₂ capture processes

A model based approach for process synthesis using highly innovative absorption solvents

Anna-Katharina Kunze, Philip Lutze, Andrzej Górak

The synthesis of gas separation processes, e.g. post combustion CO₂ capture is a challenge due to the huge variety of possible separation technologies because a dominant unit operation like distillation for liquid separations is missing. To intensify gas processing, innovative unit operations have to be taken into account, which are not state of the art in industrial application like for example enzyme-activated absorption.

Current state of the art for CO₂ separation from post combustion flue gas streams is absorption using aqueous amine solutions. Due to high costs of the solvent regeneration, there is a need for alternative methods to reduce CO₂ emissions from fossil resource based energy processes. The number of processes options is high due to the number of new materials and technologies developed for this purpose. To reduce the experimental effort, a model based approach to screen process options to improve existing technologies (like e.g. intensification of absorption using enzyme activated solvents for CO₂ capture) is applied in these studies, which will help to determine the most promising process options.

Process synthesis is carried out as a combination of a superstructure analysis, a technology database, and if necessary experiments (Fig. 1). A complex superstructure is implemented in MATLAB®, which involves all possible connections between the single operations. To reduce the computational effort, the modeling depth is fixed on short cut scale at first. After reducing the number of process options to the most promising ones, the modeling depth is enlarged and more detailed models are taken into account till a rigorous modeling is reached.

A screening of possible process options is carried out

using a technology database that provides a summary of possible technologies. In this database an overview of the process windows of each technology gives the first evaluation point for the applicability of the technology for CO₂ separation. The database comprises literature data for each investigated process, but as soon as highly innovative separation processes should be taken into account, x2 the experimental literature data becomes rare. Therefore; experimental studies have to be carried out to get information about the mass transfer characteristics of those processes e.g. to be able to model the absorption process accurately.

This method is applied to the enzyme activated absorption as an example, therefore detailed analysis of enzyme activated solvents for the absorption of CO₂ is carried out (Fig. 2). Aim of these studies is to proof, that enzyme based absorption systems show an enhanced CO₂ uptake due advantageous mass transfer kinetics of reactive solvents as well as less energy-intensive desorption. To guarantee highly accurate results the measurements are carried out following a standard method for mass transfer measurements in absorption and desorption.

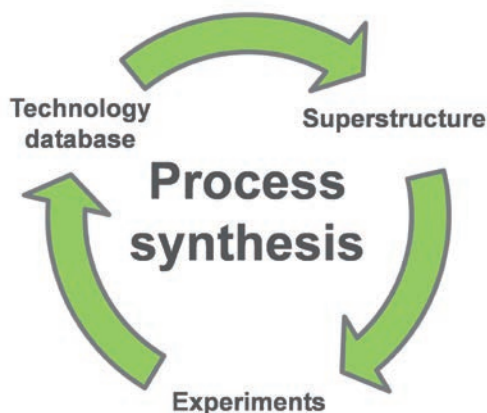


Figure 1: Tools for process synthesis.

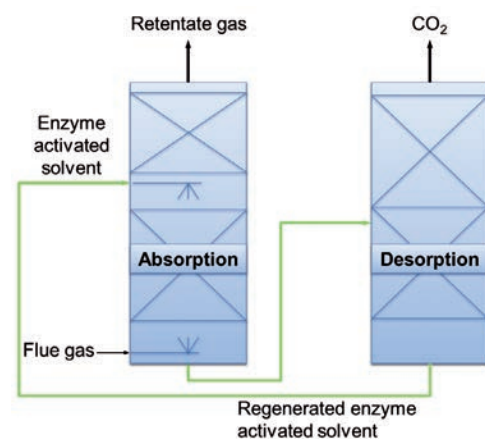


Figure 2: Absorption with enzyme activated solvents.

Contact:
anna-katharina.kunze@udo.edu.de
philip.lutze@udo.edu.de
andrzej.gorak@udo.edu.de

Publications:

A. Kunze et al., "Hybrid processing for CO₂ capture – A model based approach for process synthesis" AIChE Spring Meeting 2013, San Antonio, USA.

A. Kunze et al., „Entwicklung einer standardisierten Methodik für Stofftransportmessungen in der Ab- und Desorption“ Process-Net-Jahrestagung 2012, Karlsruhe, Germany.

Reactive Extraction

Determination of the reaction kinetics of terpenylamines in liquid-liquid-two-phase-systems

Robin Schulz, Tim Zeiner, Andrzej Górak

Terpenes, as a renewable, alternative raw material of the oil and gas based chemical industry, have a high potential for various synthesis routes. A promising synthesis is their hydroamination to terpenylamines. In this case, reactive extraction with homogeneous catalysts compared to a heterogeneously process has a significant increase in selectivity. The aim of this research is a simulation tool for the reactive extraction in liquid-liquid-two-phase-systems.

Terpenylamines are feedstock for production of polyamides based on renewable resources. They are made from terpenes, derived for example from tree resin and are already industrial available. Thus, they do not compete with food production, like many other renewable resources.

Terpenylamines are synthesized by a hydroamination of terpenes and a secondary amine. A model reaction is the conversion of β -myrcene with morpholine, catalysed by platinum (Figure 1). Since the platinum does not dissolve in myrcene it must be provided from an aqueous phase, which forms a liquid-liquid-two-phase-system with myrcene. Morpholine is distributed in both phases. Thus the reaction only takes place at the interface of the two phases.

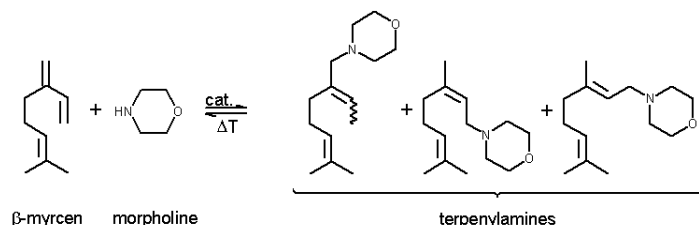


Figure 1: Hydroamination of β -myrcene with morpholine to terpenylamines using a transition metal catalyst.

For a study of such reactive liquid-liquid-two-phase-system, knowledge of the reaction order and the reaction kinetics is necessary depending on the parameters affects. We report on determination of the reaction kinetics in a Nitsch-cell (Figure 2), allowing for measurement of concentration over time is needed. The cell enables to keep constant interface between two liquid phases, with the phase formers water and myrcene, without mixing the two phases.



Figure 2: Operating Nitsch-cell with bottom aqueous phase and top organic phase with constant interfacial area consisting of double-walled glass vessel with reactor internals for both phases.

Thereby a concentration-time curve is estimated by sampling the two phases over the entire reaction period. Figure 3 shows results of a benchmark experiment with a cadmium complexation reaction.

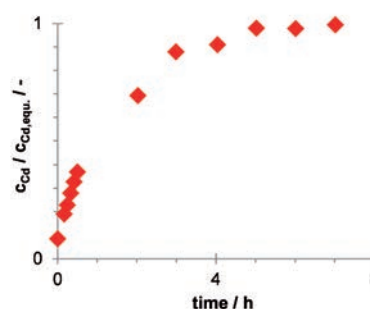
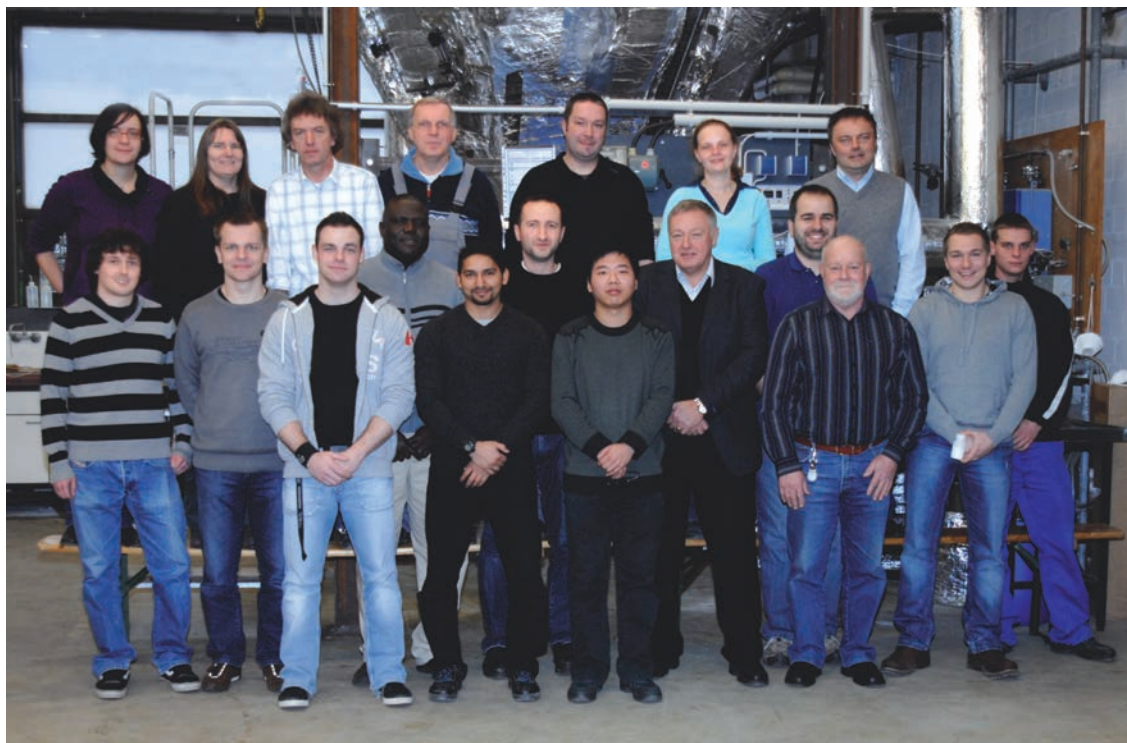


Figure 3: Plot of cadmium concentration in the organic phase over time for a period of eight hours of a benchmark experiment.

A process model will be created using the obtained reaction kinetics. Therewith an industrial process can be simulated and validated in a mixer-settler-miniplant.

Contact:
 robin.schulz@udo.edu.de
 tim.zeiner@udo.edu.de
 andrzej.gorak@udo.edu.de



Mechanical Process Engineering (MV)

Auto-conveying probing-apparatus for extraction of particle free samples from process gasses

Axel Mescher, Peter Walzel

For inline-characterization of particle laden process gasses a filtration system for keeping the analyst free of particles, is usually required. Additionally gas-pumps are needed for overcoming the pressure drop of filter-element and filter-cake. Consecutive reactions of process gas and filter-cake may be disadvantageous for the quality of the gas-analysis. A new probing apparatus is presented for extraction of particle-free gas samples from particle-laden process gasses. The probe combines the functionalities of a gas-pump and a particle separator. While the gas is transported from process to analysis, particles are separated in situ according to the principle of air classification.

The probing apparatus can be mounted to different devices of gas/solid-process, e.g. to the piping or directly to reaction devices. Only the foremost part of the probing apparatus (drilled, hollow shaft) has to be located inside the process device.

Figure 1 shows a sketch of the probing apparatus. It contains a rotor and a sealed casing. All parts were fabricated from stainless steel by lathing and drilling.

The rotor consists of a shaft of 12 mm outer diameter and a larger rotor wheel with 60 mm outer diameter. The rotor is supported by sealed ball-bearings.

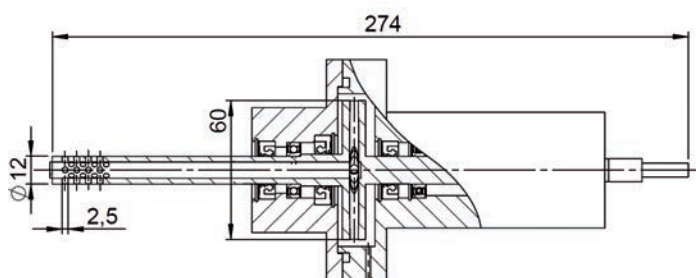


Figure 1: Sketch of the probing apparatus.

The shaft of the rotor has an axial borehole reaching from the rotor wheel to the head of the shaft, which is located inside the gas/solid-process. The shaft-head as well as the rotor wheel contain radial boreholes, in order to allow the process gas to pass the probing apparatus.

By driving the rotor an aerostatic pressure difference builds up due to the different diameters of the wheel and the head part of the shaft. The aerostatic pressure difference leads to transport of the process gas through the apparatus. The gas is extracted from the particle-laden environment and leaves the probing apparatus through a borehole in the casing of the rotor.

Due to the rotation of the forefront part of the probing

apparatus the particle load of the process-gas is deflected from the head part of the probing apparatus. The deflection of particles occurs according to the principles of air classification, which is sensitive to the particle size, revolution rate of the rotor and to the transported gas-flowrate.

Larger particles show larger ratios of centrifugal forces to air drag forces and are separated more efficiently compared to smaller particles.

When increasing the rotor revolution rate both increases, the gas-flowrate and therefore the drag forces, as well as the centrifugal forces acting on the particles. However, the separation efficiency for smaller particles with diameter x increases for higher revolution rates n according to $x \sim 1/n$.

The rotor can be chucked and driven e.g. by customary and inexpensive grinding drives. Revolution rates of 15,000 to 35,000 rpm can be typically achieved by such drives.

The ventilation characteristics as well as the separation efficiency for different particle sizes were investigated for several revolution rates of the rotor. Even at low revolution rates $< 20,000$ rpm, the probing apparatus allows for gas-flowrates of $0.1 - 0.5$ m³/h and maximum backpressures of ~ 15 mbar, both sufficient for typical gas analyzing systems. At such revolution rates particles larger than ~ 8 μ m are completely separated. Increased revolution rate n leads to higher possible backpressure, higher flowrate and to separation of finer particles.

Publications:
A. Mescher and P. Walzel,
Auto-conveying probing-apparatus for extraction of particle free
samples from process gasses,
Chem.-Ing.-Techn. (2013).

Transportation of thin fluid films by pulsation

Application of synthetic wall jets for counter-current flow contactors

Thomas Sturz, Peter Walzel

Counter-current fluid transport of two liquid phases can be achieved e.g. by gravity, pressure difference or drag as a driving force for each phase. Pressure difference is limited to very low values due to shortcut problems. Another possibility to drive counter-current flow contactors is to take advantage of jet entrainment, in particular at synthetic jets. Synthetic jets appear to be more suitable compared to continuous jets because they are generated with the working fluid and therefore concentration fluctuations inside the contactor can be avoided.

Synthetic jets arise from repeating suction and expulsion at orifices or small openings. The flow pattern induced in the surrounding fluid during suction and expulsion phases differ significantly and therefore, despite of a zero net mass flux, a net impulse is induced, even when the oscillation is harmonic. A counter-current flow contactor can be driven by an array of synthetic wall jets with orifices or openings located in series within a plate along a channel. The resulting jets entrain the ambient fluid and cause a movement of the adjacent film along the duct. First, the feasibility of a single phase flow based on this concept was tested in a synthetic wall jet drive like shown in Figure 1.

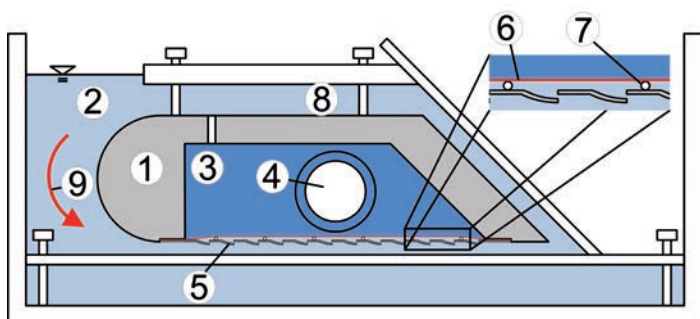


Figure 1: Experimental set-up of the synthetic wall jet drive; 1: acrylic chest; 2: working section; 3: driving section; 4: pulsation inlet; 5: Conidur® plate; 6: flexible membrane (thickness: 1 mm); 7: spacer ($d = 1$ mm); 8: PIV gap; 9: direction of induced flow.

This device consists of an acrylic chest carrying a Conidur® plate (Hein Lehmann GmbH) like shown in Figure 2 which contains 200 regular arranged inclined orifices with an equivalent diameter of $d_{\text{equ}} = 0.53$ mm. On the bottom of this plate spacer-pins and a flexible membrane

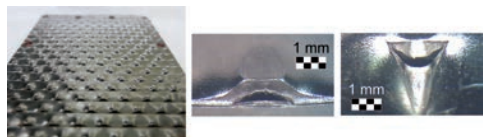


Figure 2: Orifice arrangement on the Conidur® plate and detailed view of the orifices.

are mounted creating defined compartments for synthetic wall jet generation and separating the driving section from the working section, respectively. The driving fluid (water-glycerol mixture, 10 mPas) is oscillated and transfers the oscillation to the flexible membrane via the pulsation inlet. The harmonic displacement of the membrane leads to generation of synthetic wall jets with the working fluid (water) at the orifices from the Conidur® plate. The emerging jets entrain ambient fluid, drive the film along the gap and force the liquid to flow around the chest. Like shown in Figure 3 flow induction depends on the pulsation parameters, frequency and amplitude.

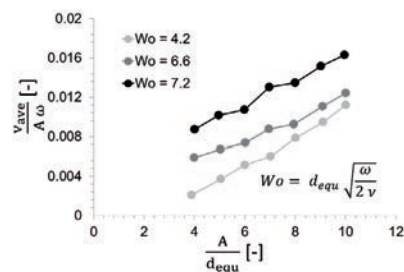


Figure 3: Efficiency of transferred oscillation energy into the system regarding flow induction by emerging synthetic wall jets out of the Conidur® plate ($W_o =$ Womersley number, v_{ave} = average velocity below the Conidur® plate; A = amplitude at the orifice).

Due to the turbulent character of the emerging synthetic wall jets, obviously a considerable amount of energy is lost by friction but simultaneously enhancing mass transport. Nevertheless, fluid transport by synthetic wall jets seems feasible. A possible solution for a counter-current flow contactor based on this concept is shown in Figure 4. Flow shortcuts between the two phases can be avoided by a perforated plate stabilizing the interface.

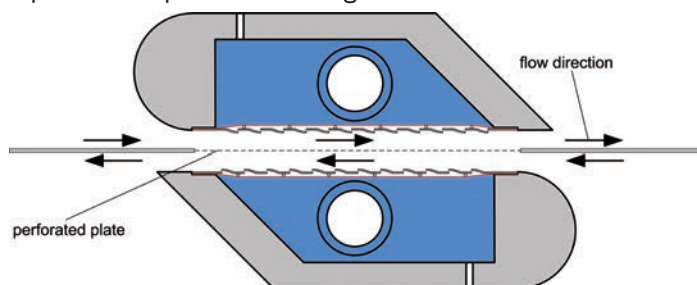
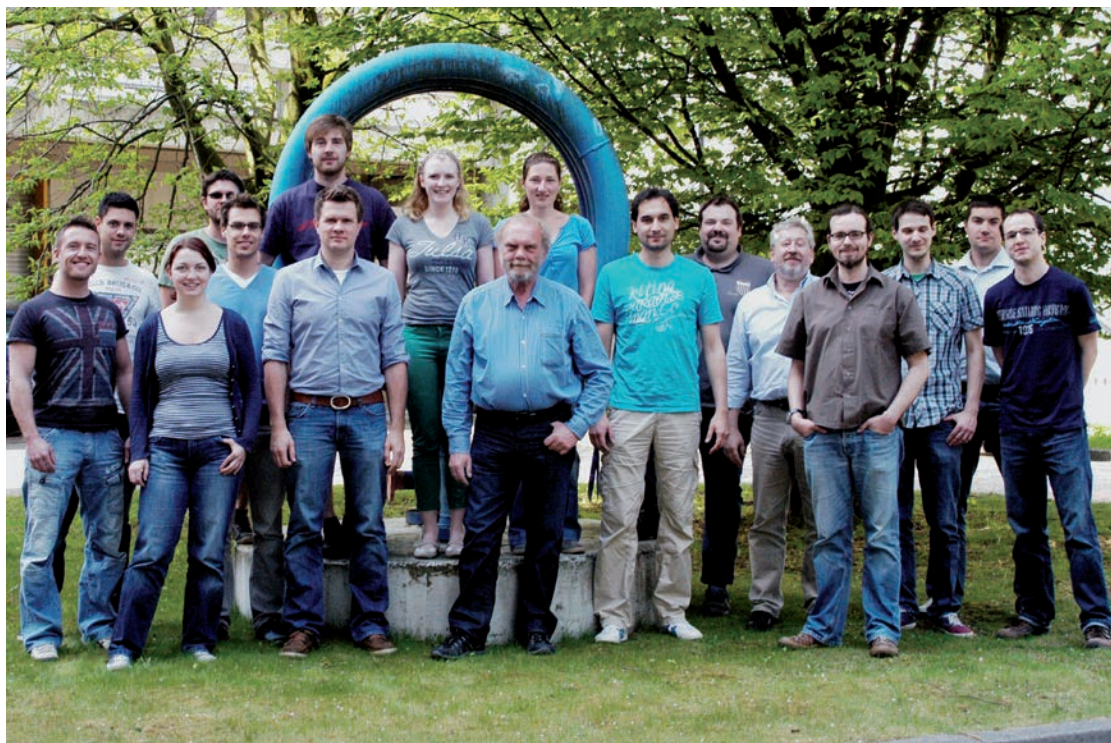


Figure 4: Counter-current flow contactor based on the Conidur® plate concept.

Contact:
thomas.sturz@bci.tu-dortmund.de
peter.walzel@bci.tu-dortmund.de





Fluid Mechanics (SM)

Microfluidics

Electrokinetic flows in microchannels with internal electrodes

Carsten Gizewski, Peter Ehrhard

In microfluidic devices, electrokinetic phenomena can be engaged to manipulate liquids, particles, or cells. In general, electrokinetic phenomena are related to the existence of electrical double layers (EDL), which are present e.g. where solid walls are in contact with electrolytes. Due to surface charges on the solid, ions of opposite charge are attracted and lead to a thin electrically non-neutral zone, the EDL. The application of an electrical field leads to forces onto the fluid inside the EDL, capable of driving a flow within the microchannel. This particular flow is termed electroosmotic. If, additionally, electrodes are placed inside the microchannel, due to small distances, strong inhomogeneous electrical fields can be induced, which in turn cause complex flow fields..

The electrokinetic flow in a microchannel with a rectangular cross section of $100\ \mu\text{m} \times 200\ \mu\text{m}$ is investigated whereas internal electrodes are placed on the top and bottom walls of the microchannel (cf. Gizewski & Ehrhard (2012)). During the experiments electrical fields are applied and the polarities of the electrodes are switched periodically. The fluid is seeded with fluorescent particles to visualize the fluid flow and the flow fields are measured using the μPIV method. With this method it is possible to measure the two components (u, v) of the velocity field which are tangential to the top and bottom walls of the microchannel. For the given configuration of electrodes, the flow features an important velocity component which is normal to the top and bottom walls. As the measurement plane is parallel to the top and bottom walls, this out-of-plane component cannot be measured directly.

To infer this out-of-plane velocity component w , a method based on the continuity equation is applied: Firstly, a set of velocity fields (u, v) at different heights of the microchannel is measured via μPIV . Secondly, based on this set, the unknown velocity component w is inferred by integrating the continuity equation in the z direction, starting at the walls.

All expressions inside the above integral can be inferred from the measured (u, v) fields. Hence, $w(x, y)$ can be computed.

$$w = - \int_0^z \left(\frac{\partial u}{\partial x} + \frac{\partial v}{\partial y} \right) dz$$

In Figure 1 and Figure 2 the measured velocity fields (u, w) in the x - z plane are given for two different polarities of the electrodes. Hereby, the velocity component w in the z direction is not measured directly, but inferred via the continuity equation. All measurements are taken 100 ms after the switch of polarity.

[1] B. Walter, P. Ehrhard, *Proc. Appl. Math. Mech. (PAMM)* 9, 31, 2009.

Contact:
carsten.gizewski@bci.tu-dortmund.de
p.ehrhard@bci.tu-dortmund.de

These experimental results clearly show a dependency of the particle movement on the electrode polarity: a switch of the polarity leads to a switch of the direction of particle movement. In contrast, the numerical simulations of the electroosmotic flow in this microchannel with internal electrodes, independent of the electrode polarities,

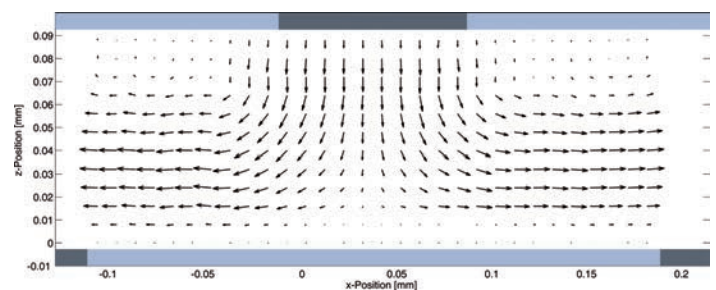


Figure 1: Velocity field (u, w) for a top electrode potential of +500 mV and a bottom electrode potential of -500 mV. The flow is directed upwards towards the top electrode.

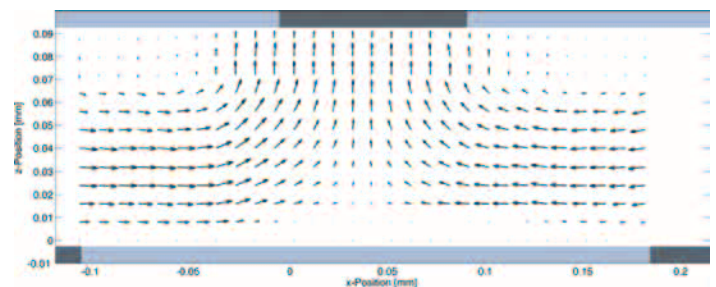


Figure 2: Velocity field (u, w) for a top electrode potential of -500 mV and a bottom electrode potential of +500 mV. The flow is directed downward from the top electrode.

always show flows directed away from the electrode center (cf. Walter & Ehrhard (2009)). This leads to the conclusion that the particle movement is caused by both, the electroosmotic fluid flow and the electrophoretic forces onto the slightly-charged particles.

Publications:
C. Gizewski, P. Ehrhard, *Proc. Appl. Math. Mech. (PAMM)* 12, 465, 2012.

Two-phase micro-reactors

Numerical study of a liquid/liquid slug flow in a capillary micro-reactor

Ina Dittmar, Peter Ehrhard

The great advantage of micro-reactors is associated with an extremely large surface-to-volume ratio. Hence, micro-reactors permit promising operating conditions, such as almost perfect heat or mass transfer. This, of course, requires that the hydrodynamics is well understood. The hydrodynamics of a liquid/liquid slug flow in a micro-capillary is characterized by a complex vortex structure in both, disperse and the continuous phase. Understanding of these complex flows allows for a control of the hydrodynamics, and thus, for a tailoring of the heat and mass transport.

We focus on a cylindrical capillary with two immiscible liquids, operated in the slug-flow regime, with a perfectly-wetting continuous phase and a non-wetting disperse phase. Consequently, there is a thin film of continuous phase separating the disperse phase from the wall. In general the slug flow can be divided in three different regions: a region of constant film thickness, a transition region, and a region of constant curvature. The dimensionless groups of this problem are a Reynolds number Re , a capillary number Ca , the dimensionless film thickness δ and the ratios of viscosities η and of densities λ (cf. Dittmar & Ehrhard (2012)). Due to the small height of the microchannel, gravity can be safely neglected. Hence, the problem can be treated in an axially-symmetric manner.

In this study we want to capture the hydrodynamics, which is mainly characterized by the flow fields within both phases and by the liquid/liquid interface position. To compute this, we engage an immersed-boundary formulation of the Navier-Stokes equations which is sketched in detail in Lakshmanan & Ehrhard (2010).

In Figure 1 we present a situation, which is strongly influenced by capillary forces, as obvious from $Ca = 10^{-3}$, and has identical viscosities and densities in both phases. Obviously, the interface is cylindrical in the middle region and spherical (and symmetric) at both ends of the disperse slug. The flow is given by one large toroidal vortex in the continuous phase and one large toroidal vortex in the dispersed phase. Additionally, there are two small toroidal vortices, located at the front, and at the back end of the disperse slug.

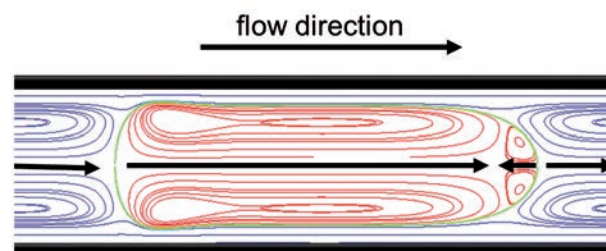


Figure 2: Streamlines for a liquid/liquid slug flow. The dimensionless groups are $\lambda = 1$, $\eta = 1$, $Re = 1$, $Ca = 0.1$ (disperse: red; continuous: blue; Interface: green).

Figure 2 shows the situation for a larger capillary number of $Ca = 0.1$, involving weak capillary forces only. Now the front cap and the rear cap of the disperse slug clearly have different spherical shapes and the interface in the middle region is no longer cylindrical. Even though the other parameters are maintained, this has an effect onto the flow: We still recognize two large toroidal vortices, both in the continuous and the dispersed phase. The small toroidal vortex located at the front end of the disperse slug is still present, while the small vortex at the back end of the slug has disappeared.

The flow patterns found in Figure 1 and Figure 2 closely resemble flow patterns found experimentally in rectangular microchannels by Miessner et al. (2008) by engaging the μ PIV technique.

U. Miessner et al., *Proc. 14th Int. Symp. Appl. Laser Techn. Fluid Mech.*, 2008.

P. Lakshmanan, P. Ehrhard, *J. Fluid Mech.* **647**, 143, 2010.

Contact:

ina.dittmar@bci.tu-dortmund.de
p.ehrhard@bci.tu-dortmund.de

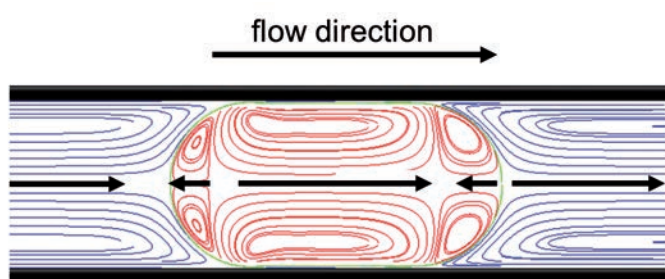


Figure 1: Streamlines for a liquid/liquid slug flow. The dimensionless groups are $\lambda = 1$, $\eta = 1$, $Re = 1$, $Ca = 10^{-3}$ (disperse: red; continuous: blue; Interface: green).

Publications:

I. Dittmar, P. Ehrhard, *Proc. Appl. Math. Mech. (PAMM)* **12**, 511, 2012.

Liquid-particle micro-flow

Numerical study of single particle motion in laminar pipe flow

Maximilian Fischer, Peter Ehrhard

Particles in a laminar pipe flow migrate radially to an equilibrium position. This so-called Segré-Silberberg effect can be engaged for the separation of particles of different size. This separation method has been introduced and successfully applied within laboratory experiments at the Chair of Mechanical Process Engineering (MVT) of TU Dortmund within the frame of a collaboration project, financed by DFG (cf. Matulka & Walzel (2011)). For the design and optimization of the separation, a precise knowledge of the equilibrium and the influencing parameters appears crucial. In our part of the collaboration project, we investigate the hydrodynamics of this equilibrium, as it depends e.g. on the particle size and on the pipe Reynolds number.

In laminar pipe (micro-) flows, particles are not only subject to drag and lift forces, but also to torque, which is due to different shear stresses at either sides of the particle (cf. Figure 1).

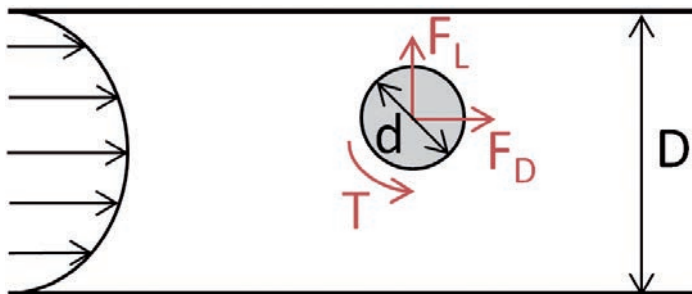


Figure 1: Forces and torque onto particles in laminar pipe flow.

Our simulation approach is based on an iterative two-loop strategy. First, the spherical particle of given diameter d is placed at a guessed radial position, and guessed values for the axial velocity and rotation rate are assigned via the boundary conditions. A stationary simulation is performed and both drag force and torque are evaluated. In an inner loop, the axial velocity and the rotation rate are adjusted until both the drag force and the torque vanish. Now, in an outer loop, the lift force is evaluated and the radial position of the particle is adjusted until the lift force vanishes. Of course, at each new radial position, the inner loop has to be re-engaged. Eventually, we find an axial velocity, a rotation rate, and a radial position, where both the force and torque onto the particle vanish – this is the equilibrium.

The commercial finite-volume code ANSYS/CFX is used as numerical tool. All simulations are carried out in a particle-fixed frame of reference. This allows for an accurate evaluation of the force and torque, acting on the particle, by exploiting stationary simulations on non-moving hexahedral grids.

Contact:
Maximilian.Fischer@bci.tu-dortmund.de
p.ehrhard@bci.tu-dortmund.de

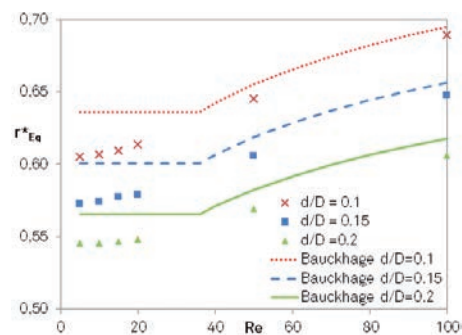


Figure 2: Dimensionless radial equilibrium position r^*_{Eq} over pipe Reynolds number Re for different particle sizes (d/D). Symbols present our data, lines present correlations based on experiments by Bauckhage (1973).

Figure 2 shows the equilibrium position r^*_{Eq} as function of the pipe Reynolds number Re for three particles of different size. Here, r^*_{Eq} represents the particle center within the equilibrium state, non-dimensionalized by the pipe radius. With increasing Re , the equilibrium position is shifted outward, from the pipe center towards the pipe wall. Moreover, larger particles find their equilibrium position closer to the pipe center. Our results appear to be in good agreement with the experiments of Bauckhage (1973). However, in the range $Re < 36$, Bauckhages experimental correlation suggests radial position, independent of Re . In contrast, our numerical investigations reveal a dependency on Re in this range.

In summary, the present approach allows for an accurate characterization of the particle equilibrium, predicting all parameters. These parameters prove to be in good agreement with available experiments in literature.

P. Matulka, X. Du, P. Walzel, *Chem. Engin. Sci.* **66**, 5930, 2011.

K. Bauckhage, Dissertation, TU Claustal, 1973.

Publications:

M. Fischer, P. Ehrhard, Numerische Untersuchung der Bewegung von Einzelpartikeln in einer laminaren Rohrströmung, *ProcessNet*, Mehrphasenströmung, Baden-Baden, 2013.



Technical Biochemistry (TB)

Localisation and detection of cannabinoids in isolated *C. sativa* L. trichomes

Nizar Happyana, Oliver Kayser

Cannabis sativa L. is an annual, dioecious herb, belonging to the family of Cannabaceae and originating from Eastern and Central Asia. Phytocannabinoids (cannabinoids), a unique group of terpenophenolics possessing alkyl-resorcinol and monoterpene moieties in their molecular structure are considered the most responsible compounds for the biological activities of *Cannabis sativa* L. (Figure 1) More than 100 cannabinoids have been identified and structurally elucidated, including recently isolated new entities. Because of their psychoactivity, Δ^9 -tetrahydrocannabinol (THC) and its related acid (Figure 2) and cannabidiol (CBD) are the most studied and interesting compounds of the class. Here we analysed by Laser Dissection Microscopy, LC-MS and LC-NMR pattern and localization of THC production in trichomes.

Trichomes, especially the capitate-stalked glandular hairs, are well known as the main sites of cannabinoid and essential oil production of *C. sativa*. In this study the distribution and density of various types of *Cannabis sativa* L. trichomes (Figure 1, right), have been investigated by scanning electron microscopy.



Figure 1: *Cannabis sativa* L. (left) and capitate stalked trichome (right).

Furthermore, glandular trichomes were isolated over the flowering period (8 weeks) by laser microdissection (LMD) (Figure 3) and the cannabinoid profile analyzed by LCMS. Cannabinoids were detected in extracts of less than 200 cells collected cells of capitate-sessile and capitate stalked trichomes and separately in the gland (head) and the stem of the latter. Δ^9 -Tetrahydrocannabinolic acid (THCA), cannabidiolic acid (CBDA), and cannabigerolic acid (CBGA) were identified as most-abundant compounds in all analyzed samples while their decarboxylated derivatives, Δ^9 -tetrahydrocannabinol (THC), cannabidiol (CBD), and cannabigerol (CBG), co-detected in all samples, were present at significantly lower levels. Cannabichromene (CBC) along with cannabiol (CBN) were identified as minor compounds only in the samples of intact capitate-stalked trichomes and their heads harvested from 8-week old plants. Cryogenic nuclear

Contact:
 nizar.happyana@bci.tu-dortmund.de
 oliver.kayser@bci.tu-dortmund.de

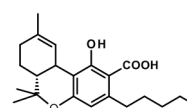


Figure 2: Δ^9 -tetrahydrocannabinolic acid (THCA).

magnetic resonance spectroscopy (NMR) was used to confirm the occurrence of major cannabinoids, THCA and CBDA, in capitate-stalked and capitate-sessile trichomes. Cryogenic NMR enabled the additional identification of cannabichromenic acid (CBCA) in the dissected trichomes, which was not possible by LCMS as standard was not available. The hereby documented detection of metabolites in the stems of capitate-stalked trichomes indicates a complex biosynthesis and localization over the trichome cells forming the glandular secretion unit.

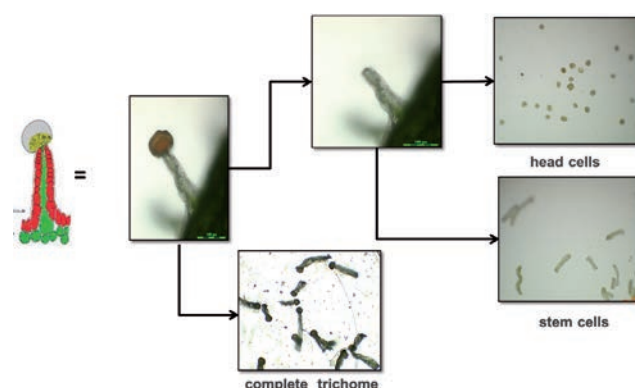


Figure 3: Schematic view on the laser dissection of trichomes from *C. sativa* L.

Publications:
 Happyana, N., Agnolet, S., Schneider, B., Kayser, O. (2012) Analysis of cannabinoids in laser microdissected trichomes of medicinal *Cannabis sativa* using LCMS and cryogenic NMR. *Phytochemistry* 87:51-59.
 Happyana, N., Muntendam, R., Kayser, O. (2012) Metabolomics as bioanalytical tool for characterization of medicinal plants and their phytomedicinal preparations, in *Pharmaceutical Biotechnology* 2nd ed. (eds. Kayser, O., Warzecha, H.) pp. 527-552.

Endophytes – the plant-associated microbial treasure troves

Elucidating the interspecies and multispecies cost-benefit crosstalks of endophytes harbored in *Cannabis sativa* L.

Parijat Kusari and Oliver Kayser

Our work focuses on understanding and elucidating the multifaceted cost-benefit tradeoffs between endophytes harbored in Cannabis sativa L. and interacting organisms (such as host-specific phytopathogens) that lead to desired biological functions (such as the production of defensive compounds that can be used as pharmaceutically relevant pro-drugs). This will enable the practical and efficient use of endophytes as biocontrol agents for plant protection against a plethora of phytopathogens, and further as competent microbial factories of bioactive natural products.

Beyond the generalized understanding of plants as multicellular organisms capable of performing photosynthesis, is a much more complex veracity of comprehending them. This includes commanding the network of associations of plants with other organisms, various biotic and abiotic selection pressures, an assortment of cost-benefit mutualisms, and interaction-directed coevolution of attack-defense-counterdefense mechanisms. A central 'partner' within these strata of natural acquaintances is a class of remarkably diverse group of microorganisms (fungi and bacteria) called endophytic microorganisms (known as endophytes). They inhabit living, internal tissues of plants, and retain a discreet association with their associated hosts for at least a part of their life (Fig. 1).

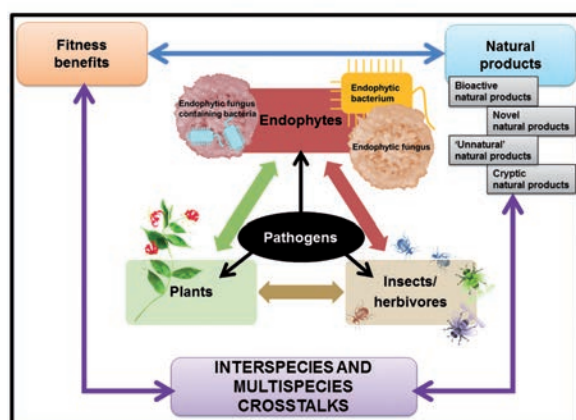


Figure 1: Schematic representation of the interspecies and multispecies crosstalks between endophytes (bacteria and fungi), pathogens, plants and feeders.

Our investigation focuses on isolation, microbiological and phylogenetic characterization, diversity evaluation, and assessment of biocontrol potential of endophytes harbored in the medicinal plant, *Cannabis sativa* L.

In spite of the production of secondary metabolites like cannabinoids, *C. sativa* suffers epidemic disasters and greenhouse destructions due to the attack of numerous phytopathogens. The total eradication and/or prevention of diseases are still open to further investigation. We have focused on the two major phytopathogens, namely *Botrytis cinerea* and *Trichothecium roseum*, known to cause grey mold and pink rot diseases in *C. sativa*. We devised dual culture setups to challenge the endophytes with these two phytopathogens in different culture conditions and parameters to evaluate the different attack-defense ecological strategies and biochemical fingerprints utilized by the endophytes in thwarting these host-specific phytopathogens.

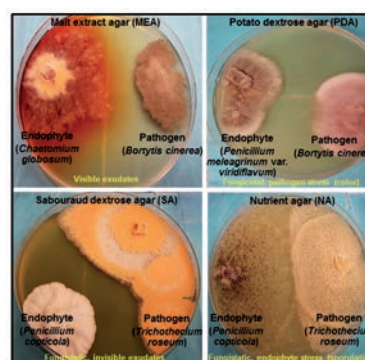


Figure 2: Representative types of *C. sativa* L. endophyte-pathogen interactions observed in dual culture antagonistic assay.

This study led to the establishment of various attack-defense-counterdefense interactions between competent endophytes and the challenging phytopathogens (Fig. 2).

Further investigation will be made for chemical elucidation of bioactive target and/or non-target compounds correlating to the endophyte-pathogen interactions, enabling us to elucidate the bio- and chemo-diversity of Cannabis-associated endophytes.

Collaborators: Souvik Kusari (s.kusari@infu.tu-dortmund.de) and Michael Spiteller (m.spiteller@infu.tu-dortmund.de), Institute of Environmental Research (INFU) of the Faculty of Chemistry of TU Dortmund.

Contact:
Parijat.kusari@bci.tu-dortmund.de
Oliver.kayser@bci.tu-dortmund.de

Publications:

- Kusari P., Kusari S., Spiteller M., Kayser O. (2012) Endophytic fungi harbored in *Cannabis sativa* L.: Diversity and potential as biocontrol agents against host plant-specific phytopathogens. *Fungal Divers.* In Press (doi: 10.1007/s13225-012-0216-3).
- Kusari P., Kusari S., Spiteller M., Kayser O. (2012) Endophytic diversity of pharmaceutically important *Cannabis sativa*. *Planta Med.* 78, 1154-1154. [Abstract for poster presented at the International Congress on Natural Products Research (ICNPR 2012), the 8th Joint Meeting of AFERP, ASP, GA, PSE and SIF; New York, USA].
- Kusari P., Spiteller M., Kayser O., Kusari S. (2013) Recent advances in research on *Cannabis sativa* L. endophytes and their prospect for the pharmaceutical industry. In: Kharwar R.N. (ed.) *Endophytes*, (ICPMB 2012), Springer-Verlag, Heidelberg. In Press.



Technical Chemistry – Chemical Process Development (TC)

Oxygen depolarized cathodes with electrodeposited catalyst

A new method to save expensive catalyst metals for oxygen reduction

Philipp Frania, Jakob Jörissen

Chlor-alkali electrolysis for the production of chlorine and caustic soda is one of the biggest consumers of electrical energy. By using oxygen depolarized cathodes (ODC) instead of classical hydrogen evolving cathodes 30% of electrical energy can be saved. Bayer MaterialScience AG – leading partner in a research project of companies and universities including TU Dortmund – has successfully put a demonstration plant of 20'000 t/y chlorine capacity into operation. The applied ODCs are based on silver catalyst. A new electrochemical method for ODC construction can decrease the content of expensive catalyst. The target of our research is the optimization of catalyst distribution varying multiple parameters of silver electrodeposition.

The oxygen reduction reaction in oxygen depolarized cathodes is only possible if three phases – oxygen gas, the electrolyte sodium hydroxide solution and electrically contacted silver – stay in direct contact. As the solubility of oxygen in sodium hydroxide solutions is low only in thin films of electrolyte on the catalyst the reaction is enabled. (Figure 1)

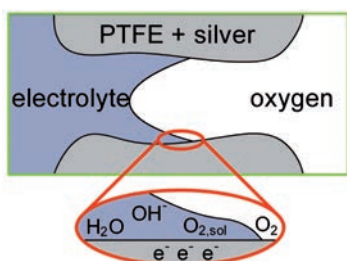
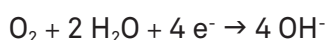


Figure 1: Principle of a gas diffusion electrode. Only where the three phases stay in contact, the oxygen can diffuse into the NaOH solution and the reaction is possible.

Oxygen depolarized cathodes are manufactured according to the state of the art by rolling a porous layer containing a mixture of silver particles and polytetrafluoroethylene (PTFE). The hydrophobic PTFE guarantees an oxygen gas phase within the porous electrode. The silver catalyst as a hydrophilic component ensures the presence of electrolyte as well as the electrical contact. But the biggest part of silver particles is agglomerated and flooded by NaOH solution and therefore most of the silver doesn't take part in the oxygen reduction reaction.

The novel gas diffusion electrodes are manufactured electrochemically. In a microporous PTFE membrane silver whiskers are deposited. While operating as ODC these silver structures are covered with a thin film of caustic soda solution. Thereby the whiskers participate in the oxygen reduction reaction using their full length. (Figure 2)

Contact:

philipp.frania@bci.tu-dortmund.de
jakob.joerissen@bci.tu-dortmund.de

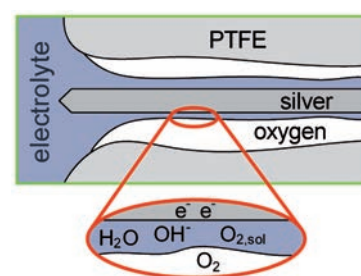


Figure 2: Principle of the novel whisker gas diffusion electrode. The silver whiskers participate in the oxygen reduction using their total surface area.

For the manufacturing process, a conductive mesh is used as cathode. On this mesh the PTFE membrane is placed and filled with an electrolyte for silver deposition. If a current between cathode and silver anode is applied silver structures are deposited along the electrical field lines. (Figure 3)

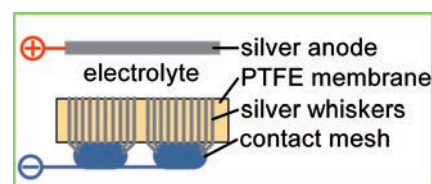


Figure 3: Manufacturing of novel whisker gas diffusion electrodes.

Main fields of research are to ensure a strong contact between mesh and silver whiskers, to increase the number of unagglomerated silver structures and to optimize the size of catalytic active material.

Actually manufactured ODCs operate in oxygen reduction with a current density higher than 6 kA/m². Scanning electron microscopy (SEM) and electrochemical analysis show a high optimization potential for silver structures and thus for ODC performance.

Publications:

Erf.: Jörissen, J.; Polcyn, G.; Toepell, G.; Verfuß, F.,
„Sauerstoffverzehrelektrode und Verfahren zu ihrer Herstellung“,
20.09.2012, Bayer IP GmbH., EP000002573212A2.

Generating primary amines in an aqueous biphasic medium

Reductive Amination of Citronellal with Ammonia

Andreas Wintzer, Arno Behr

Amines are well known for their wide application in different parts of our life today. Especially primary aliphatic fatty amines represent high quality products in chemical industry. They provide useful properties for application and are also important intermediates for further chemistry. The generation of primary amines often is a difficult undertaking, because they are good nucleophiles and can cause undesired side reactions. Homogeneous catalysis is a useful instrument for an atom economic synthesis of amines in general. One specific way to primary amines is the reductive amination of the renewable monoterpene citronellal which is presented in this work.

Using aqueous ammonia solution provides quick condensation of the substrate and the two phase solvent system (water/toluene) offers an easy separation of the product from the active catalyst species. Condensation of citronellal with ammonia yields the aldimine which is further hydrogenated to the desired primary products (Figure 1). As side products citronellol (through hydrogenation of the starting material) and secondary as well as tertiary amines can be generated.

A conversion-time plot (Figure 2) shows that the formation of the secondary imine is nearly as fast as the citronellal conversion. The hydrogenation of the primary aldimine and the anew condensation with citronellal therefore follow immediately on the condensation of the starting material with ammonia. Besides, long reaction times are switching selectivity between primary products, resulting in high yields of 80 % of the fully hydrogenated primary amine.

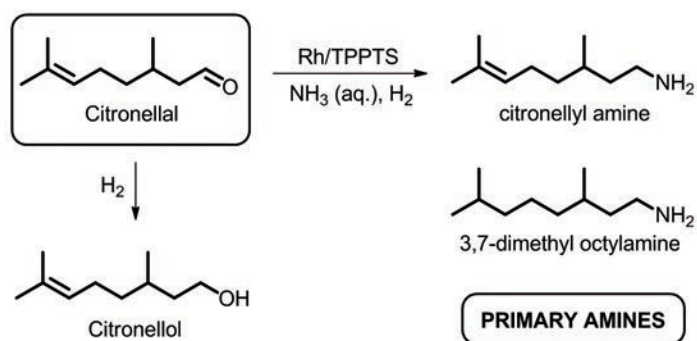


Figure 1: Reaction scheme of the reductive amination of citronellal with ammonia: major products are the primary amines, not shown are secondary and tertiary amines. (TPPTS = Triphenylphosphine trisulfonate).

The key step in this synthesis is the reverse reaction from the secondary imine which is build as side product. Therefore, a large excess of ammonia is required to provide enough cleavage activity of the undesired secondary product. The formation of tertiary amines and citronellol can be avoided by choice of optimized reaction conditions. Parameters such as precursor properties, temperature and the kind of phase transfer agent can be used as instruments.

Reductive amination of citronellal with NH₃: Conversion-time plot

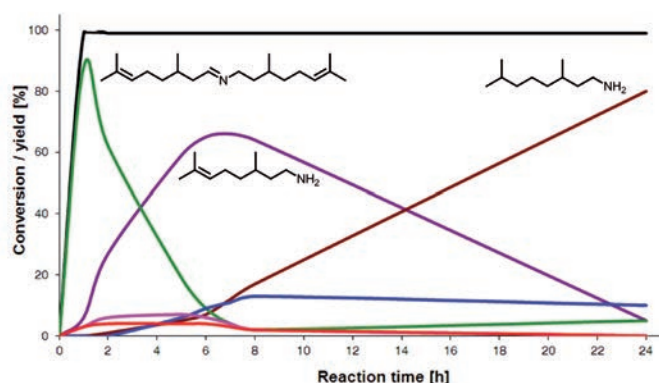


Figure 2: Conversion-time plot of the reductive amination of citronellal with ammonia: fast formation of secondary imine and its cleavage to primary products.

Due to the fact that biphasic solvent systems are subject to mass transport problems, phase transfer agents are necessary to provide high activity in this system. Besides cyclodextrins also classical surfactants, gemini surfactants and ionic liquids have useful properties for this application. They all provide high selectivity of primary amines, but differ in terms of phase separation. With surfactants such as cetyltrimethylammonium bromide (CTAB) the formation of emulsions complicates fast and accurate phase separation. With cyclodextrins (best system: methyl- β -cyclodextrin) and ionic liquids (best system: 1-methyl-3-decylammonium bromide) phase separation proceeds even faster with a well defined interface.

Contact:
arno.behr@bci.tu-dortmund.de
andreas.wintzer@bci.tu-dortmund.de

Publications:
Behr, A., Wintzer, A., Lübke, C., Müller, M., The reductive amination of citronellal with ammonia: primary amines through biphasic homogeneous catalysis, in preparation, (2013).

Ethenolysis of castor oil derivatives

Synthesis of valuable oleochemical key substances

Stephanie Krema, Alexander Kämper, Arno Behr

In the ethenolysis of the renewable raw material ricinoleic acid methyl ester the valuable oleochemical key substance methyl dec-9-enoate is produced. The products are accessible under mild reaction conditions and with the use of only small amounts of a commercial available homogeneous ruthenium catalyst. Detailed optimization leads to high conversion and yield of the desired product. Similar results were observed with the use of ricinoleic acid and castor oil as starting materials, without previous purification of the substrate.

The described reaction of ricinoleic acid methyl ester (1) is a pressure- and temperature-dependent equilibrium reaction according to the pathway in Figure 1. In parallel, however, the self metathesis to the long chain products (4) and (5) can take place.

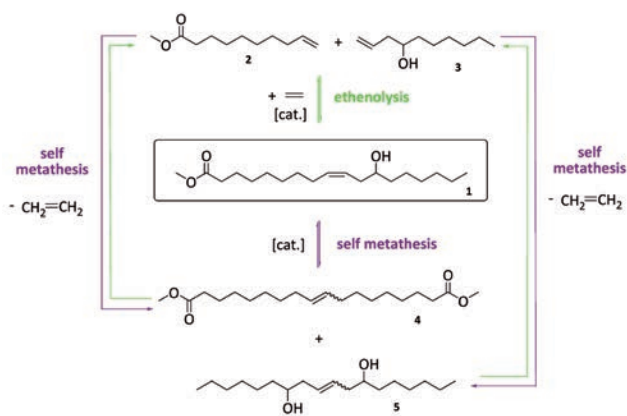


Figure 1: Ethenolysis and self metathesis of ricinoleic acid methyl ester (1).

Ethenolysis products have versatile application possibilities because of their terminal double bonds, also the by-products that result from the self metathesis can be preceded to value chemicals.

The first step of the reaction optimization was the catalyst screening; several homogeneous ruthenium complexes were investigated. A commercial available catalyst containing a phenylindenyliene complex was the most active one and was used for detailed further investigations.

In the investigation of the catalyst concentration it was remarkable that over the investigated range (0.05 – 1.5 mol%), high conversions and yields are achieved. Moreover, a steady decrease in the desired ethenolysis products (2) and (3) was observed with increasing catalyst concentration.

Further specific investigations in the variation of solvent, the solvent amount, the temperature-effect, the pressure of ethene, time experiments as well as long time experiments with low catalyst amounts were carried out. At mild reaction conditions ($t = 3$ h, $c_{\text{cat}} = 0.1$ mol%, $p = 20$ bar ethene, $T = 80$ °C) a conversion of ricinoleic acid methyl ester (1) of 99% and yields of the metathesis product (2) of 83% and (3) of 77% were observed. This corresponds to a TON of 900 and a TOF of 0.091 s⁻¹. The use of these optimized conditions for the reaction of ricinoleic acid (6) and with castor oil (8) (see Figure 2) showed similar positive results.

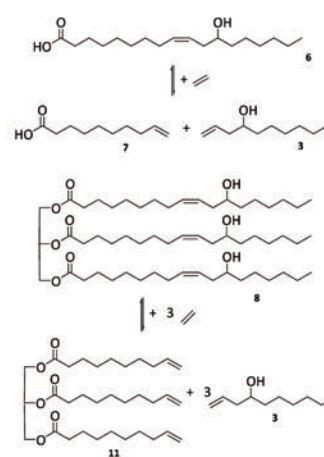


Figure 2: Ethenolysis of ricinoleic acid (6) and castor oil (8).

The described reaction offers access to well-known products with an alternative interesting raw material. Overall, castor oil derivatives are promising substrates for ethenolysis as an alternative to other fats and fatty derivatives. Due to the presence of the hydroxyl group in the products, this type of homogeneous metathesis has great potential for further use in chemical industry.

Publications:

A. Behr, S. Krema, A. Kämper, RSC Advances 2012, 2, 12775-12781
 "Ethenolysis of ricinoleic acid methyl ester – an efficient way to the oleochemical key substance methyl dec-9-enoate".

Contact:

arno.behr@bci.tu-dortmund.de

stephanie.krema@bci.tu-dortmund.de

Linear oligomerization of 1-butene with a homogeneous catalyst system based on allylic nickel complexes

Arno Behr, Zeynep Bayrak (TU Dortmund), Stefan Peitz, Guido Stochniol (Evonik Industries)

The oligomerization of 1-butene with a nickel-based catalyst system represents an elegant synthesis method for obtaining linear octenes from readily available chemicals. In literature it is well known that the so named Lodewick-catalyst ($\text{Ni}(\text{COD})(\text{hfacac})$) can be used for dimerization of 1-butene yielding 75-83% of linear octenes at high reaction temperatures of 70-80°C.[1] Now we have shown for the first time that it is also possible to use allylic nickel complexes, such as the methallyl nickel chloride dimer $[\text{Ni-1}]$, in combination with 1,1,1,5,5,5-hexafluoroacetylacetone (hfacac) to produce linear octenes with a selectivity of 70% at very mild reaction conditions and low catalyst concentrations.

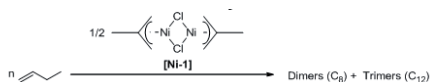


Figure 1: Oligomerization of 1-butene.

The oligomerization of 1-butene leads to the formation of different octenes. One of the major and most desired isomers are the linear octenes. After hydroformylation and subsequent hydrogenation to the alcohols they can be used for example as plasticizer for PVC as their phthalic acid esters. Other occurring isomers are the branched dimers 3-methylheptenes and the 3,4-dimethylhexenes. A key reason for the building of the branched dimers is that the 1-butene dimerization can occur by different insertion ways. A constellation of all possible insertion ways are summarized in figure 2.

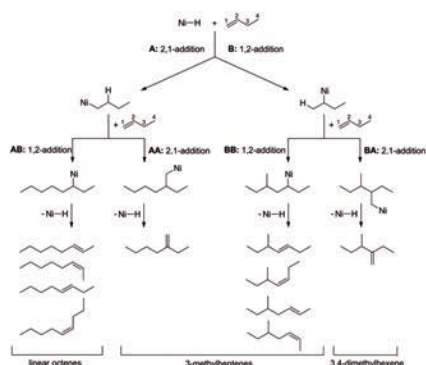


Figure 2: Insertion ways of 1-butene in oligomerization reactions with catalytic active nickel hydrides.

At the beginning of our investigations an activator screening was carried out. The activator is very important for this reaction, because it leads to the forming of the catalytic active nickel hydride species and increases the catalyst activity of the allylic nickel complex. The highest yield of 41% dimers (C_8) was investigated with hfacac, wherein 70% are linear octenes. Comparing the

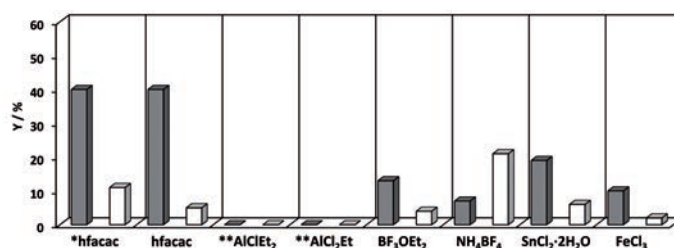


Diagram 1: Results of the activator screening

($c([\text{Ni-1}]) = 1 \text{ mol\%}$, $n(\text{activator})/n([\text{Ni-1}]) = 1$, solvent = dcm, $w(\text{solvent})/w(1\text{-Butene}) = 5$, $T = 30^\circ\text{C}$, $rt = 24 \text{ h}$, * = $\text{Ni}(\text{COD})(\text{hfacac})$, $T = 70^\circ$, solvent = toluene; ** = solvent toluene; ■ $\text{Y}(\text{C}_8)$, □ $\text{Y}(\text{C}_{12})$)

oligomerization activity of $[\text{Ni-1}]$ with the Lodewick-catalyst we obtain a similar activity. Whereas $[\text{Ni-1}]$ is already active at low reaction temperatures as 30°C and the Lodewick-catalyst has a very low activity under 70°C . The dimer yield with the Lodewick-catalyst is 41% at a reaction temperature of 70°C .

A further important influence factor is the $n(\text{hfacac})/n([\text{Ni-1}])$ -ratio. The results of these reactions show that a $n(\text{hfacac})/n([\text{Ni-1}])$ -ratio below and higher 1 lead to an

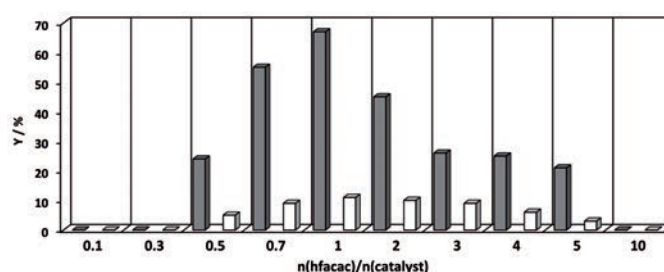


Diagram 2: Influence of the activator concentration

($c([\text{Ni-1}]) = 1 \text{ mol\%}$, solvent = dcm, $w(\text{solvent})/w(1\text{-Butene}) = 2$, $T = 30^\circ\text{C}$, $rt = 24 \text{ h}$; ■ $\text{Y}(\text{C}_8)$, □ $\text{Y}(\text{C}_{12})$)

decrease of the dimer yield. A reason for the decrease at low hfacac concentrations is that the activation of the nickel complex does not occur completely. In contrast to that high concentrations of hfacac lead to a catalyst blocking. The highest yield of 67% dimers was obtained at a $n(\text{hfacac})/n([\text{Ni-1}])$ -ratio of 1.

[1] R. Lodewick, "Über lineare Oligomerisierung von Olefinen, Dissertation Aachen, 1977.

[2] G. Wilke, B. Bogdanovic, W. Keim, "Allyl Übergangsmetallsysteme", *Angew. Chem.* **1966**, *3*, 157.

Contact:

arno.behr@bci.tu-dortmund.de

zeynep.bayrak@bci.tu-dortmund.de

Publications:

Posters Presentation at the "46. Jahrestreffen Dt. Katalytiker" in Weimar, 13.-15.03.2013

Title: "Linear Oligomerization of 1-butene with a homogenous catalysed system based on allylic nickel complexes"; A. Behr, Z. Bayrak, S. Peitz, G. Stochniol.

Enantioselective Tandem Reactions at Elevated Temperatures

One-Pot Hydroformylation/S_N1 Alkylation

Karoline A. Ostrowski, Andreas J. Vorholt, Julian Stiller, Arno Behr, Mathias Christmann

Catalytic tandem reactions describe a reaction sequence with two or more catalytic reactions in a single reaction vessel, thereby minimizing solvents, purification and costly material transfers between reaction steps.

The first orthogonal tandem hydroformylation/ α -alkylation of simple and functionalised olefins with alcohols providing high yields and excellent enantioselectivities is presented (Fig. 1). As model substrates for the desired tandem reaction, 1 hexene (**1a**) as active terminal olefin and alcohol **2** as carbocation precursor were chosen.

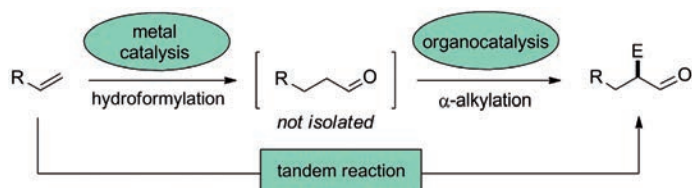


Figure 1: Tandem transition metal catalysed hydroformylation/ organocatalytic α -alkylation (E = electrophile).

For the hydroformylation, a rhodium/ruthenium complex and a phosphine ligand (DPPB) were selected and synthesis gas (1:1) pressure of 30 bars was applied. An organocatalyst was used for the α alkylation (Fig. 2) with additional acid for carbocation generation.

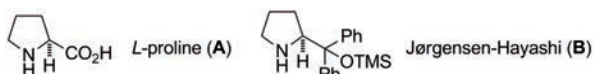


Figure 2: Selection of applied organocatalysts.

Some selected results for the developed orthogonal tandem catalysis are presented (Fig. 3 & Tab. 1).

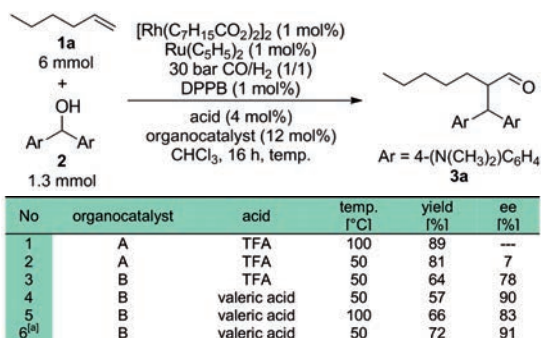


Figure 3, Table 1: TFA = trifluoroacetic acid, DPPB = 1,4-bis(diphenylphosphino)butane. [a] 12 mol% valeric acid. [b] Yield determined by GC analysis.

An excess of **1a** afforded **3a** in 89% (entry 1). Lower reaction temperature results in lower yield (entry 2). L-proline gave virtually no enantioselectivity. Catalyst **B** comprises a high-yielding and highly enantioselective tandem catalysis, because of its bulky phenyl and TMS groups.

Contact:

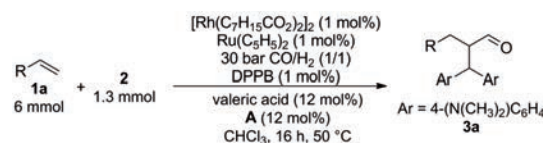
karoline.ostrowski@bci.tu-dortmund.de
andreas.vorholt@bci.tu-dortmund.de
julian.stiller@gmx.net
arno.behr@bci.tu-dortmund.de
mathias.christmann@tu-dortmund.de

The best results were obtained with weak acids like valeric acid (entry 4) increasing the ee.

Elevated temperatures led to lower enantioselectivities but higher yields. Nevertheless, it is remarkable for an organocatalytic reaction that high enantioselectivities of 83% ee were obtained at 100 °C (entry 5).

A proposal for the mechanism of organocatalytic α alkylation suggests a direct participation of the acid in the cation formation. Increasing the amount of acid resulted in higher yields without effecting the ee (entry 6).

In order to test the scope and limitations of this tandem reaction, we applied the optimized reaction conditions to a variety of commercially available olefins (Fig. 4 & Tab. 2).



No	olefin	yield ^[a] [%]	ee [%]
1	1c	62	92
2	1d	43	93
3	1e	85	93 (93) (d.r. 1/1)
4	1f	83	83
5	1g	76	98 (80) (d.r. 3/1)

Figure 4, Table 2: [a] Isolated yield after column chromatography. d.r. = diastereomeric ratio.

Linear (entry 1), aromatic (entry 2), cyclic (entry 3), hydroxy- (entry 4) and diene- functionalised (entry 5) olefins underwent this tandem catalysis with high enantioselectivities and yields.

In this work, we have established an orthogonal tandem hydroformylation/ α -alkylation to yield chiral α -substituted aldehydes with high enantiomeric excess up to 98%. The tandem reaction is also extendable to more complex alkenes and to substrates with additional functional groups.

Publications:

J. Stiller, A. J. Vorholt, K. A. Ostrowski, A. Behr, M. Christmann, Chem. Eur. J. 2012, 18, 9496-9499 „Enantioselective Tandem Reactions at Elevated Temperatures: One-Pot Hydroformylation/SN1 Alkylation“.



Thermodynamics (TH)

Modelling of hydrogel networks

A thermodynamic method for the description and prediction of smart polymers

Markus C. Arndt, Gabriele Sadowski

Hydrogels are networks of highly hydrophilic polymer chains that can swell and absorb immense amounts of solvents. For their thermodynamic modeling elastic forces were implemented in the PC-SAFT equation of state and the resultant elastic pressure in such gels was explicitly considered. This way, the influence of the external stimuli temperature, pressure and concentrations on the swelling behavior of hydrogels could be correlated to experimental data and a significant predictive character of the model was proven.

Due to their affinity to hydrophilic solvents, cross-linked hydrogel polymers are excellent super-absorbers. For a special representative among hydrogels, poly(N-isopropylacrylamide) PNIPAAm, this swelling capability can be triggered by external stimuli: by variation of the temperature or addition of certain solutes or co-solvents the highly swollen polymer undergoes an abrupt but fully reversible transition and shrinks dramatically by nearly full loss of the previously stored solvent. This feature characterizes the biocompatible PNIPAAm systems as smart polymers and opens a wide field of promising applications such as in the biomedical sector as triggerable drug depot or sensor/actuator in microfluidic systems.

Next to the model parameters of PNIPAAm we determined binary-interaction parameters, for which a prediction approach could be developed. With these, not only general thermodynamic behavior of aqueous PNIPAAm solutions such as vapour-liquid or liquid-liquid equilibria could be calculated, but the swelling of PNIPAAm hydrogels was modeled considering the elastic-energy contribution. Here, the response of gel systems to pressure and temperature changes was successfully described as well as the influence of various additional substances such as alcohols, acetone, poly(ethylene glycol) or diverse salts. Figure 1 and Figure 2 show the dramatic swelling/shrinking transition triggered by temperature and composition changes.

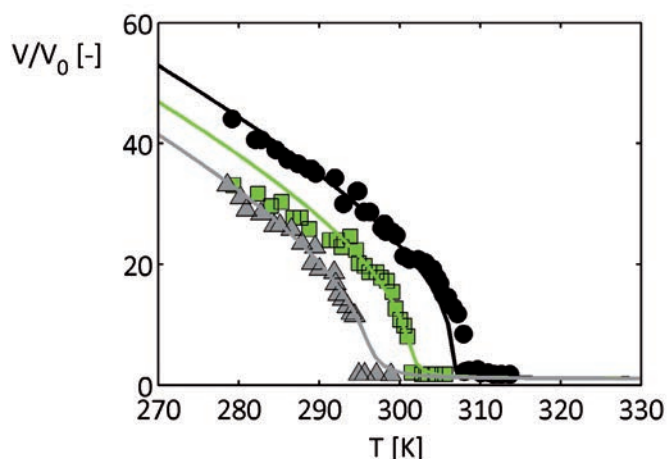


Figure 1: The temperature-triggered swelling calculation (lines) of the PNIPAAm hydrogel in aqueous NaCl solution with increasing salt concentration (black: 0.0 M; green: 0.5 M, grey: 1.0 M) in comparison with experimental data (symbols). The swelling is given as gel volume V in reference to the dry gel volume V_0 .

The thermodynamic evaluation of such swellable polymer systems was performed with the PC-SAFT equation of state with explicit consideration of the elastic energy: by water molecule diffusion into the gel the cross-linked polymer chains are stretched and analogue to an elastic spring react with a counteracting contracting force. In addition to and as consequence of this elastic energy, the pressure increases strongly within the gel phase.

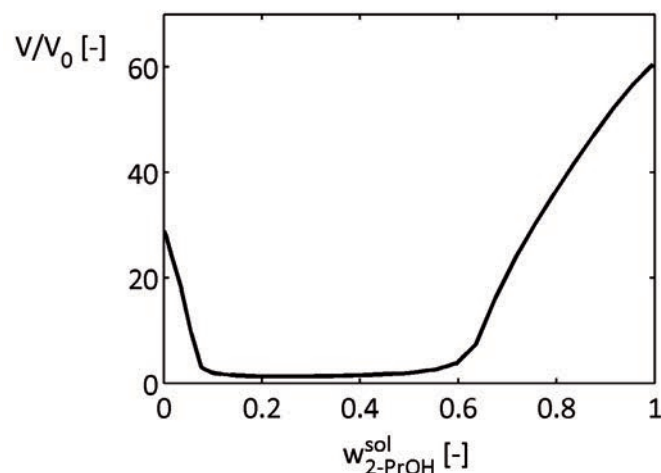


Figure 2: At constant 25 °C in the water/2-propanol system, the model gives a strong influence of the alcohol concentration in the solution phase on the PNIPAAm gel swelling: in the pure solvents gels are swollen, while strongly shrunken at propanol weight fractions in the sol phase between 0.1 and 0.6.

Contact:
markus.arndt@bci.tu-dortmund.de
gabriele.sadowski@bci.tu-dortmund.de

Publications:
M. C. Arndt, G. Sadowski, *Macromolecules* 2012, 45, 6686-6696.
M. C. Arndt, G. Sadowski, *Progress in Colloid and Polymer Science* 2013, accepted.

Thermodynamics of biological reactions

Philip Hoffmann, Matthias Voges, Christoph Held, Gabriele Sadowski

The thermodynamics of biological reactions can be analyzed in terms of Gibbs energies of reaction (Δ^Rg) or equilibrium constants. In this project, it was demonstrated that these key quantities may be heavily affected by the reactant and product activity coefficients. For the hydrolysis of methyl ferulate, these activity coefficients strongly deviate from unity (the value which is usually assumed), causing a deviation of up to 40% in the Δ^Rg values.

Genomically-possible reactions or pathways in a metabolic network are constrained by the Second Law of Thermodynamics. This connects the change in Gibbs energy of reaction (Δ^Rg) to the feasibility of reactions. However, the application of thermodynamics as currently carried out obviously neglects several important factors that certainly influence the Gibbs energy of reaction and thus yields questionable results concerning the reaction feasibility.

The hydrolysis of methyl ferulate (Fig. 1) was used as a model reaction to investigate the most relevant factors affecting Δ^Rg .

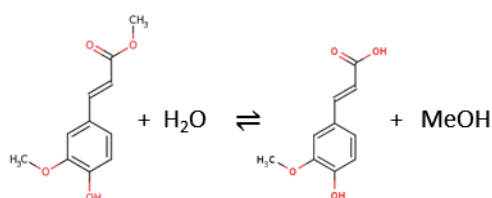


Figure 1: Hydrolysis of methyl ferulate (MF) to ferulic acid (FA) and methanol (MeOH).

Reaction-equilibrium measurements have shown that apparent equilibrium constants K_m depend strongly on the initial MF concentration (see Fig. 2) and on the excess of MeOH. This can only be explained by non-ideal reactant and product activity coefficients (Fig. 2), which are usually neglected so far. However, thermodynamic equilibrium constants K_a (Eq. 1) have to be used for the calculation of Δ^Rg values (instead of concentration-based equilibrium constants K_m) according to

$$K_a = K_m \cdot K_\gamma \quad \text{Eq. 1}$$

where K_γ is the ratio of product and reactant activity coefficients. Furthermore, it was shown in this work that K_γ values can be determined using the thermodynamic model PC-SAFT. Accordingly, it is possible to predict unknown K_a values of reactions where 'only' K_m values were measured (and where reactant and product concentration are reported).

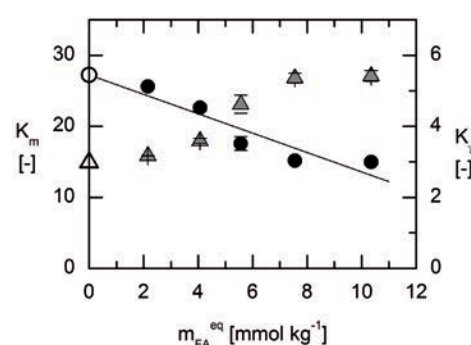


Figure 2: Equilibrium constants K_m (circles, left ordinate) and reactant activity coefficient ratio K_γ (triangles, right ordinate) of methyl ferulate hydrolysis as a function of the ferulic acid equilibrium molality. The product of K_m^∞ (open circle) and K_γ^∞ (open triangle) yields the thermodynamic equilibrium constant K_a .

Moreover, possible operation windows (ratio of reactant (MF) and product (FA) molalities which ensure that the reaction proceeds forward) were calculated (Fig. 3). It was found that the range of possible MF and FA molalities is strongly increased upon the consideration of activity coefficients.

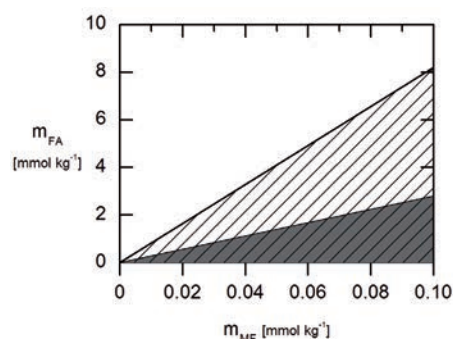


Figure 3: Possible operation windows for methyl ferulate hydrolysis calculated with (striped area) and without considering activity coefficients (dark gray area).

The results demonstrate that more realistic Δ^Rg values for feasibility studies can be obtained if reactant and product activity coefficients are explicitly accounted for.

Publications:
P. Hoffmann, M. Voges, C. Held, G. Sadowski, Biophysical Chemistry 2013, 173-174, 21-30.

Contact:
philip.hoffmann@bci.tu-dortmund.de
matthias.voges@bci.tu-dortmund.de
gabriele.sadowski@bci.tu-dortmund.de
christoph.held@bci.tu-dortmund.de

Thermodynamic Characterization of Ionic Liquid Solutions

Investigation of binary and ternary systems for 1-butanol extraction from aqueous solutions

Alexander Nann, Christoph Held, Gabriele Sadowski

In biochemical and chemical processes, ionic liquids (ILs) show an enormous potential as agents for the extraction of 1-butanol from diluted aqueous solutions. In this work, activity-coefficient data of 1-butanol/IL mixtures were measured and modeled with PC-SAFT. These data qualitatively rate the affinity of an IL to 1-butanol. PC-SAFT was then successfully used to quantitatively predict the liquid-liquid equilibria (LLE) of ternary solutions containing 1-butanol, water, and an IL. Significant properties required for designing extraction process (distribution coefficients and selectivities) were also well predicted.

Ionic liquids (ILs) are organic salts that usually consist of a large organic cation and a small inorganic anion. One example is shown in Figure 1. The enormous variety of possible anion-cation combinations allows for the development and design of task-specific ILs ("tailor-made components").

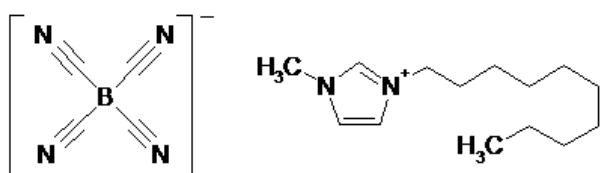


Figure 1: Ions of the IL 1-decyl-3-methyl-imidazolium tetracyanoborate ([Im10.1]⁺[tcb]⁻).

The activity-coefficient data of four binary 1-butanol/IL solutions have been determined experimentally using the techniques vapour-pressure osmometry (VPO), headspace-gas chromatography (HS-GC), and gas-liquid chromatography (GLC) (see Figure 2). These methods allow for obtaining experimental data over the entire IL concentration range.

The lower the 1-butanol activity coefficients, the higher are the (1-butanol)-IL interactions. Analyzing the activity-coefficient data the following trend for the (1-butanol)-IL interactions was obtained for the ILs studied: [Im10.1]⁺[tcb]⁻ > [Mo10.1]⁺[tcb]⁻ > [Im10.1]⁺[ntf2]⁻ > [Mo10.1]⁺[ntf2]⁻. The highest (1-butanol)-IL interactions were found for [Im10.1]⁺[tcb]⁻; thus [Im10.1]⁺[tcb]⁻ showed the highest affinity for 1-butanol compared to the other ILs investigated in this work.

It can be seen from Figure 2 that the experimental data can be described accurately using the thermodynamic model PC-SAFT.

As the aim of this work was to consider extraction systems, the LLE of ternary 1-butanol/water/IL systems was measured and modeled. As Figure 3 shows, the experimental data and the PC-SAFT predictions are in excellent agreement. That is, without fitting any

additional parameters to these data PC-SAFT is able to predict the tie lines and the binodal curve accurately. Furthermore, distribution coefficients and selectivities were calculated from the experiments. The modelling of these properties yielded also good agreement to the data.

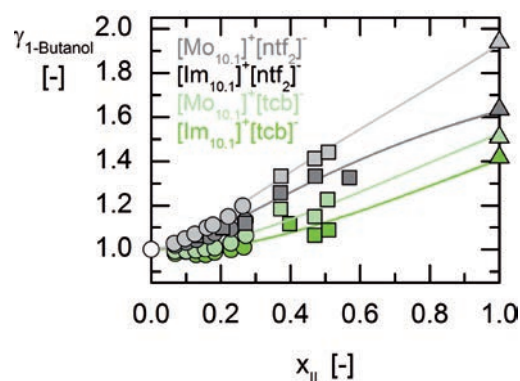


Figure 2: Activity coefficients $\gamma_{1\text{-Butanol}}$ of 1-butanol as a function of the IL mole fraction in binary solutions with IL at 323.15 K. Symbols: experimental data (VPO (circles), HS-GC (squares), GLC (triangles)), lines: PC-SAFT.

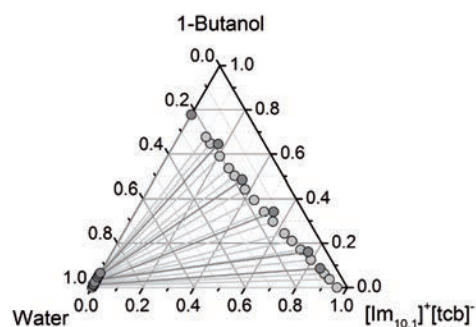


Figure 3: Predicted tie-lines for the ternary LLE 1-butanol/water/[Im10.1]⁺[tcb]⁻ (in mass fraction). Light grey: PC-SAFT, dark grey: experimental data.

Contact:

alexander.nann@bci.tu-dortmund.de
christoph.held@bci.tu-dortmund.de
gabriele.sadowski@bci.tu-dortmund.de



Publications:

A. Nann, C. Held, J. Mündges, S. P. Verevkin, G. Sadowski, The Journal of Physical Chemistry 2013, 117, 3173-3185.

Integrated Chemical Processes in Liquid Multiphase Systems (InPROMPT)

Collaborative Research Centre (DFG-Sonderforschungsbereich) Transregio 63

The Transregional Collaborative Research Center InPROMPT is a cluster of research projects that spans over several universities and institutions: Technische Universität Berlin, Technische Universität Dortmund, Otto-von-Guericke-Universität Magdeburg, ETH Zürich and Max-Planck-Institut für Dynamik komplexer technischer Systeme/ Magdeburg.

More than 60 scientists are working interdisciplinarily on the fast development of new chemical production processes which involve several liquid phases. The focus of research is not only on the reaction step but – in a holistic spirit – the entire process chain from raw material to the pure product is dealt with to attain an integral and fast process development. In InPROMPT, a technical approach that is not much used in industry yet is pursued: the application of solvent systems with tunable properties in chemical reactions. The long-term goal is to optimize such liquid-liquid systems. As a model reaction, the rhodium catalyzed hydroformylation of 1-dodecene (see figure 1) was chosen for the integral process development.

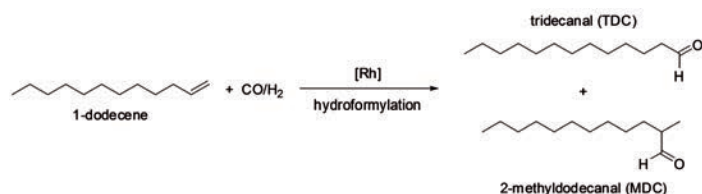


Figure 1: Hydroformylation of 1-dodecene.

Five groups of the department are working within InPROMPT: TC (Prof. Behr), TH (Prof. Sadowski), FVT (Prof. Górak), APT (Prof. Schembecker) and DYN (Prof. Engell). The collaboration of the research groups (figure 2) is illustrated in figure 3.

The **APT and DYN groups** develop a method and a computer program for the support of the development of novel chemical processes by which information about the economic performance of alternative flowsheets is given based on uncertain information on the performance of the single steps.

The **TC group** investigates the hydroformylation process on the lab scale and in a continuously driven miniplant including an efficient catalyst recycling via thermomorphic multicomponent solvent systems.

The **FVT group** investigates the separation of wide and close boiling mixtures using hybrid separations, consisting of distillation, crystallization and organic solvent nanofiltration (OSN).

The **TH group** measures and models the thermodynamic behavior and phase equilibria of the reaction systems containing solvents and reactants. Moreover, a process for separating the aldehyde isomers via melt crystallization is developed.

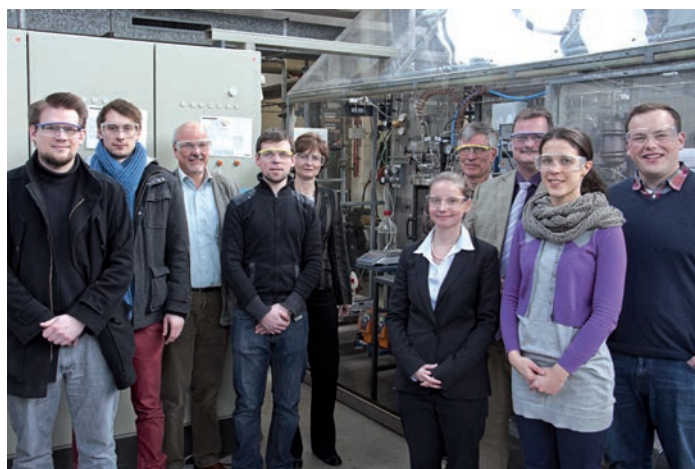


Figure 2: Research Group at TU Dortmund.

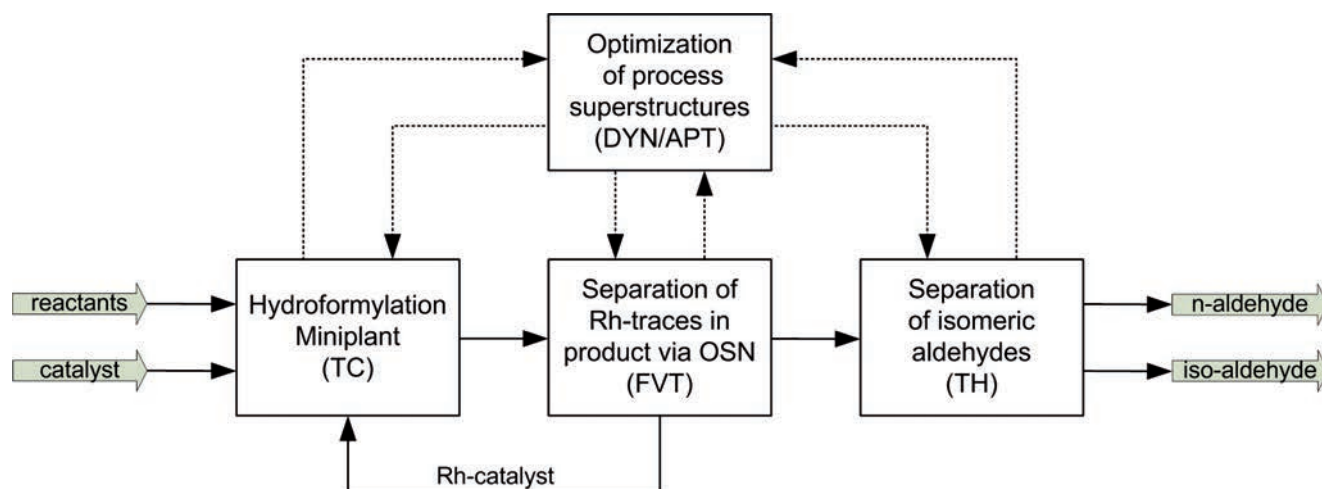


Figure 3: Collaboration of the research groups within our department.

A framework for the modeling and stochastic optimization of process superstructures under uncertainty

Jochen Steimel, Marius Harrmann, Gerhard Schembecker, Sebastian Engell

Despite many efforts to formalize the early phase of conceptual process design, no tool-supported systematic method for the conceptual design of chemical processes has been developed to date. This contribution presents a methodology and a software tool for the early conceptual design phase, which is characterized by limited and uncertain information on the available process units. The proposed methodology supports the graphical modeling of hierarchical superstructures which are subsequently optimized by a hybrid evolutionary algorithm considering uncertainty in model parameters.

The early phases of chemical process design are often characterized by a lack of information, uncertainty in the available information and a huge number of possible alternatives. In this contribution novel applications for the optimization under parametric uncertainty are presented. In our approach uncertainties are described by an interval bounding the values observed by the experiments. In this case study the energy price, the activation energy and an equilibrium constant have been considered as uncertain. The uncertainties were discretized in three levels and composed into scenarios, in order to approximate the uncertainty space.

The computational paradigm used for the optimization of design alternatives is two-stage-stochastic programming. The idea behind this method is the decomposition of the set of design variables into two subsets.

The first stage variables contain the structural design decisions inherent in chemical process design: the number and connectivity of process units, discrete design parameters such as number of stages in a column and continuous design parameters such as the volume of reactors. The second stage variables contain operational

degrees of freedom such as temperatures, pressures and flow rates. The salient feature of two-stage-stochastic programming is to adapt the values of the second-stage variables after the uncertainties are resolved, in order to react to changed process conditions. Thus an optimal operating point of the plant is computed for each scenario and taken into account in the evaluation of the design.

The method has been implemented in the computer framework FSOpt, which provides an integrated development environment for process superstructures and optimization problems. A tailored memetic algorithm integrates the state-of-the-art NLP solver IPOPT into an evolutionary framework to provide an efficient method for the solution of mixed-integer nonlinear problems.

Our method was applied to a superstructure of the C12 hydroformylation process, which is depicted in Figure 1. In this case study the primary uncertainty was identified as the phase distribution of the expensive Rhodium-based catalyst in the decanter unit. The optimized design consists of a CSTR, a decanter, an organophilic nanofiltration membrane, a crystallizer and two vacuum distillation columns.

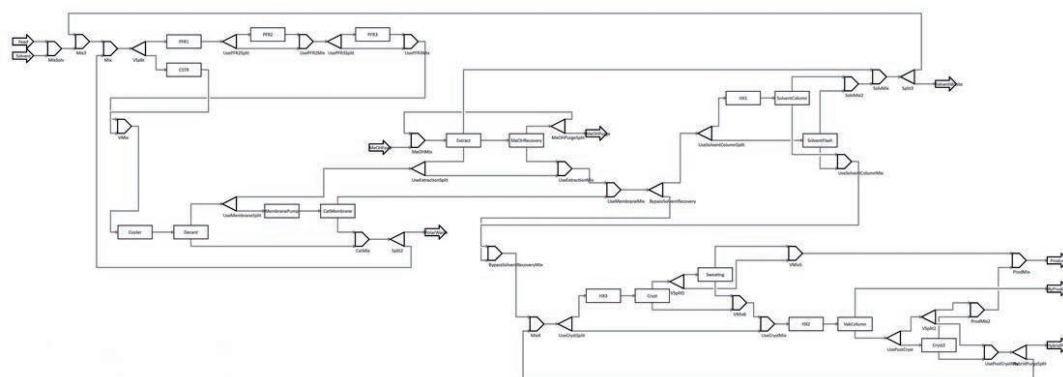


Figure 1: Superstructure of the hydroformylation process.

Contact:
jochen.steimel@bci.tu-dortmund.de
s.engell@bci.tu-dortmund.de

Publications:

- [1] Steimel, J.; Harrmann, M.; Schembecker, G.; Engell, S. Model-based Conceptual Design and Tool Support for the Early Stage Development of Chemical Processes, *Computers and Chemical Engineering*, accepted.
- [2] Steimel, J.; Harrmann, M.; Schembecker, G.; Engell, S. A framework for the modeling and optimization of process superstructures under uncertainty, *Chemical Engineering Science*, DOI:10.1016/j.ces.2013.04.052.

Graphical design tools for Organic Solvent Nanofiltration

Utilising multi-component membrane characterisation for conceptual process design

Patrick Schmidt, Philip Lutze, Andrzej Górak

Organic Solvent Nanofiltration (OSN) is a pressure-driven membrane separation process which has a large potential to complement energy-demanding unit operations. However, its industrial application is limited. Reasons for that are very limited data on the performance of commercial membranes and a lack of understanding in the underlying permeation mechanism. To gain more insight into both, we developed graphical tools that can be used in conceptual phases of process design. These include membrane rejection maps (MRM) to highlight rejections in different solvent mixtures and membrane modelling maps (MMM) to highlight recommended measures for rejection improvement.

To demonstrate the new graphical tools, we investigated the influence of the solvent mixture on the rejection of five dissolved solutes, using the polyimide-based commercial OSN membranes Starmem™122 and Puramem™280. As standard solvents, toluene, n-hexane and 2-propanol were chosen as representatives for aromatics, alkanes and alcohols. As solutes, two alkanes, two alkyl benzenes and one ligand were used. The rejections of the solutes in different binary and ternary solvent mixtures were analysed using cross-flow OSN lab-scale experiments. In order to highlight the rejection trends, isolines of same rejections were plotted in ternary diagrams as function of the applied solvent mixtures, referred to as MRM (Figure 1).

Moreover, a phenomena-based permeation model was developed based on two phenomena: Solution-diffusion and pore-flow. Moreover, solvent-solute-membrane interactions were taken into account. Based on experimental rejection data in binary solvent mixtures, model parameters were estimated and the shares of the transport phenomena were calculated accordingly. To highlight the dominating transport phenomena (either being dominated by pore-flow or solution-diffusion), membrane modelling maps (MMM) were introduced. Based on the simulated shares of the permeation phenomena, MMM plot in ternary diagrams the recommended measures to improve solute rejection.

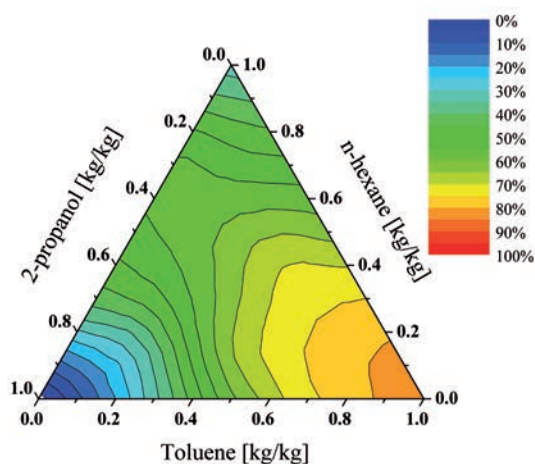


Figure 1: MRM of 1-phenyldodecane through Starmem™122 at 30bar highlighting rejections [%], using ternary mixtures of toluene, n-hexane and 2-propanol.

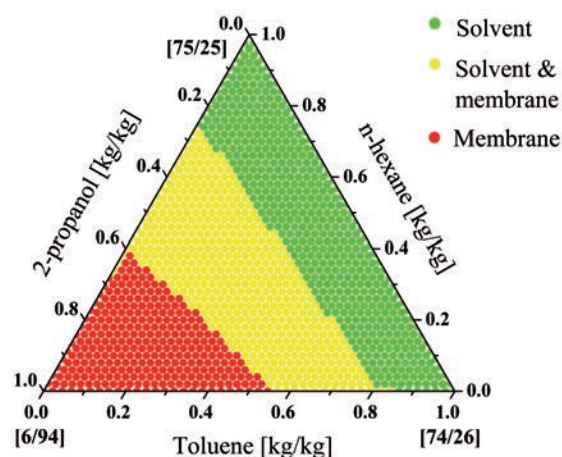


Figure 2: MMM of 1-phenyldodecane through Starmem™122 at 30bar highlighting recommended measures for rejection improvement, using ternary mixtures of toluene, n-hexane and 2-propanol.

For an example of an MMM, see Figure 2.

In conclusion, MRM and MMM can be used to support the conceptual design process for OSN in the future. During the research, the tools were validated on two industrial case studies. Moreover, the tools can be easily applied to other membrane separation processes by plotting other performance criteria, e.g. membrane selectivity, in ternary diagrams.

Publications:
P. Schmidt, T. Köse, P. Lutze, J. Memb. Sci., 429, 2013, 103-120,
DOI: 10.1016/j.memsci.2012.11.031.
P. Schmidt, P. Lutze, J. Memb. Sci., 2013, Article in Press
DOI: 10.1016/j.memsci.2013.05.062.

Contact:
patrick.schmidt@udo.edu.de
philip.lutze@udo.edu.de
andrzej.gorak@udo.edu.de

Rhodium Catalyzed Hydroformylation of 1-Dodecene

Design and Construction of a Continuously Operated Miniplant

Michael Zagajewski, Jens Dreimann, Arno Behr

This work is part of the Collaborative Research Centre Transregio 63 „Integrated chemical processes in liquid multiphase systems“ (InPROMPT), which investigates methodologies for the development of efficient production processes based on chemical reactions in liquid multiphase systems. These methodological studies are carried out using the hydroformylation of 1-dodecene (Fig. 1) as a model reaction with the use of thermomorphic or micellar solvent systems.

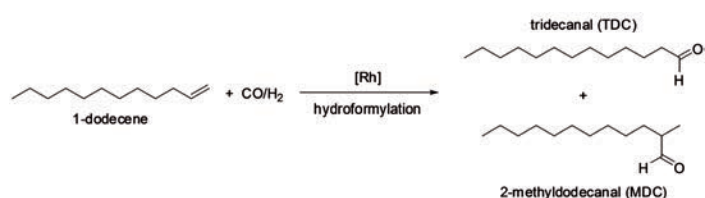


Figure 1: Hydroformylation of 1-Dodecene.

The challenging task of the homogeneously catalyzed hydroformylation of higher olefins is an efficient combination of the reaction and a separation step for catalyst recovery and recycling. In this work, a fully automated continuous process for the hydroformylation of 1-dodecene with special regard to an efficient catalyst recycling is designed, constructed and investigated (Figure 2).

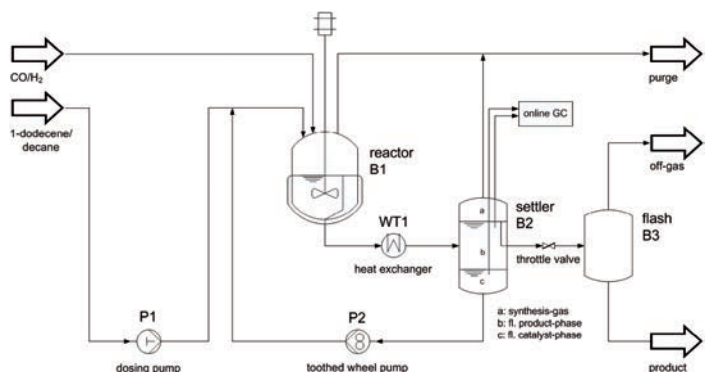


Figure 2: Miniplant Setup.

By using a thermomorphic solvent (TMS) system the reaction step can be performed homogeneously without mass transfer limitations at high temperature. Decreasing the temperature in the separation step leads to the formation of a liquid-liquid two phase system, which consists of a catalyst and a product rich phase. By means of the miniplant technique long term investigation of

catalyst stability is possible in the early phase of process development. Continuous operation provides a means for monitoring of the recycle streams in the process in order to locate accumulation of impurities and byproducts.

A highly flexible miniplant has been designed and constructed for the continuous hydroformylation of long-chain olefins (Figure 3). Preliminary studies of residence time distribution were done and the mean residence time was determined for different feed rates. Using Rh(acac)(CO)₂ and the bidentate Biphephos ligand the reaction was performed with the model substrate 1-dodecene in a thermomorphic multicomponent solvent system consisting of dimethylformamide and decane. The catalyst recycling concept was successfully validated in numerous long term operations without loss of rhodium activity. High selectivity towards tridecanal with l/b-ratios of 99:1 was achieved at conversions higher than 70 %.



Figure 3: Miniplant at the Chair of Technical Chemistry.

The financial support from the Deutsche Forschungsgemeinschaft (DFG) is gratefully acknowledged. We thank the Umicore AG & Co. KG for the donation of the rhodium precursor.

Contact:

Michael.Zagajewski@bci.tu-dortmund.de
Jens.Dreimann@bci.tu-dortmund.de
Arno.Behr@bci.tu-dortmund.de

Publications:

A. Behr, H. Witte, M. Zagajewski, "Scale up via Miniplant-Technique: Examples of Homogeneous Catalysis", Chem. Ing. Tech., 2012, 84, 5, 694-703.

M. Zagajewski, A. Behr, "Continuously Operated Miniplant for the Rhodium Catalyzed Hydroformylation of 1-Dodecene in a Thermomorphic Multicomponent Solvent System (TMS)", submitted.

Melt crystallization of isomeric long-chain aldehydes

Separating industrially highly relevant products from hydroformylation processes

Thorsten Beierling, Gabriele Sadowski

The hydroformylation of long-chain olefins, an industrially highly-relevant reaction, produces a mixture of isomeric long-chain aldehydes. The purified aldehydes are used as bulk and fine chemicals. Due to small differences in boiling points, conventional methods for their separation and purification like stand-alone distillation tend to be costly or even infeasible. Layer melt crystallization in contrast is a technically proven and selective method for separating isomeric compounds. This work shows the huge potential of melt crystallization for the separation of isomeric long-chain aldehydes. Furthermore, a model was developed which is able to predict crystal growth rates as function of process conditions without the use of any fitted parameter.

Three fundamental informations have to be known for the development of crystallization processes: 1) the solid-liquid equilibria, 2) the growth rates as function of process conditions, and 3) the respective achievable crystal purities.

Concerning the thermodynamics of the solid-liquid equilibrium, it could be shown that isomeric aldehydes form eutectic mixtures where the respective linear aldehyde is the conveniently-crystallizable compound (see figure 1).

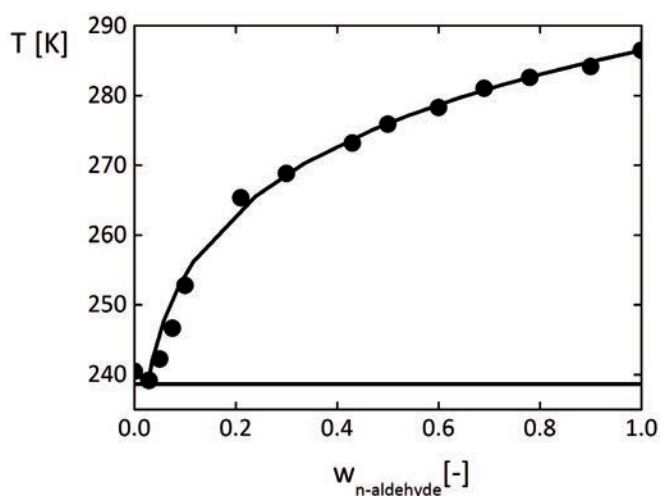


Figure 1: Solid-liquid equilibrium of the binary aldehyde mixture n-dodecanal/ iso-dodecanal.

Crystal growth rates were measured in static layer melt crystallization experiments as function of cooling rate and initial melt concentration (see figure 2). Based on the physical description of heat and mass transport, a model was developed that is able to predict the growth rates without the use of any fitted parameters (see figure 2).

The grown crystals could be extensively further purified by the post-purification step sweating. Here, the temperature of the crystal is set closely beneath the melting temperature. As a consequence, impurities adherent at the crystal and present in the crystal melt, fractionally dilute with the pure component and drain out.

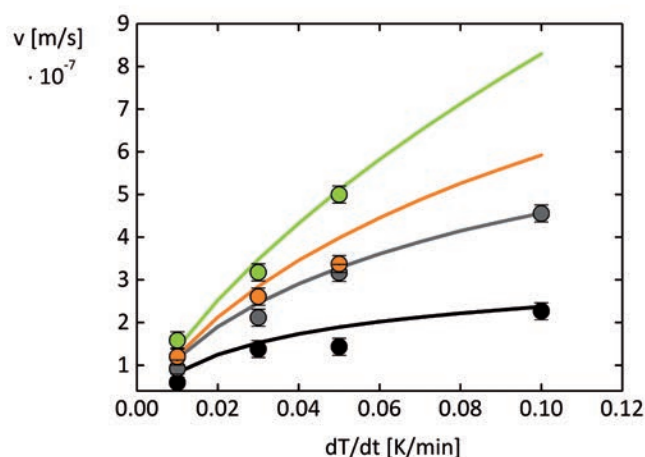


Figure 2: Measured (symbols) and predicted (lines) growth rates of the isomeric aldehyde mixture n-dodecanal/iso-dodecanal as a function of cooling rate at four different melt concentrations (black: $w_n=0.55$; grey: $w_n=0.8$; orange: $w_n=0.9$; green: $w_n=1.0$).

Starting from initial melt concentrations of 80 wt% of n-aldehyde, crystal purities up to 98.5 wt% were achieved, which is a tremendous separation efficiency for melt crystallization processes. In conclusion, melt crystallization is a very promising method to separate commercially highly relevant isomeric long-chain aldehyde mixtures and it is clearly advisable to consider melt crystallization as the method of choice for this separation task.

This work is part of the DFG Sonderforschungsbereich Transregio 63 (SFB/TR 63) InPROMPT. Financial support by the Deutsche Forschungsgemeinschaft (DFG) is gratefully acknowledged.

Publications:
T. Beierling, F. Ruether, Chemical Engineering Science, 2012, 77, 71-77.
J. Micovic, T. Beierling, P. Lutze, G. Sadowski and G. Górak, Chemical Engineering and Processing: Process Intensification, 2012, DOI: 10.1016/j.cep.2012.07.012.

Contact:
thorsten.beierling@bci.tu-dortmund.de
gabriele.sadowski@bci.tu-dortmund.de

Impressum

Fakultät Bio- und Chemieingenieurwesen
der Technischen Universität Dortmund
Prof. Jörg C. Tiller
Emil-Figge-Str. 66
44227 Dortmund
www.bci.tu-dortmund.de

SCIENTIFIC

HIGHLIGHTS